Cosmic-ray anti-helium nuclei or the quest for antimatter in the Universe

Pierre Salati – LAPTh & Université Savoie Mont Blanc

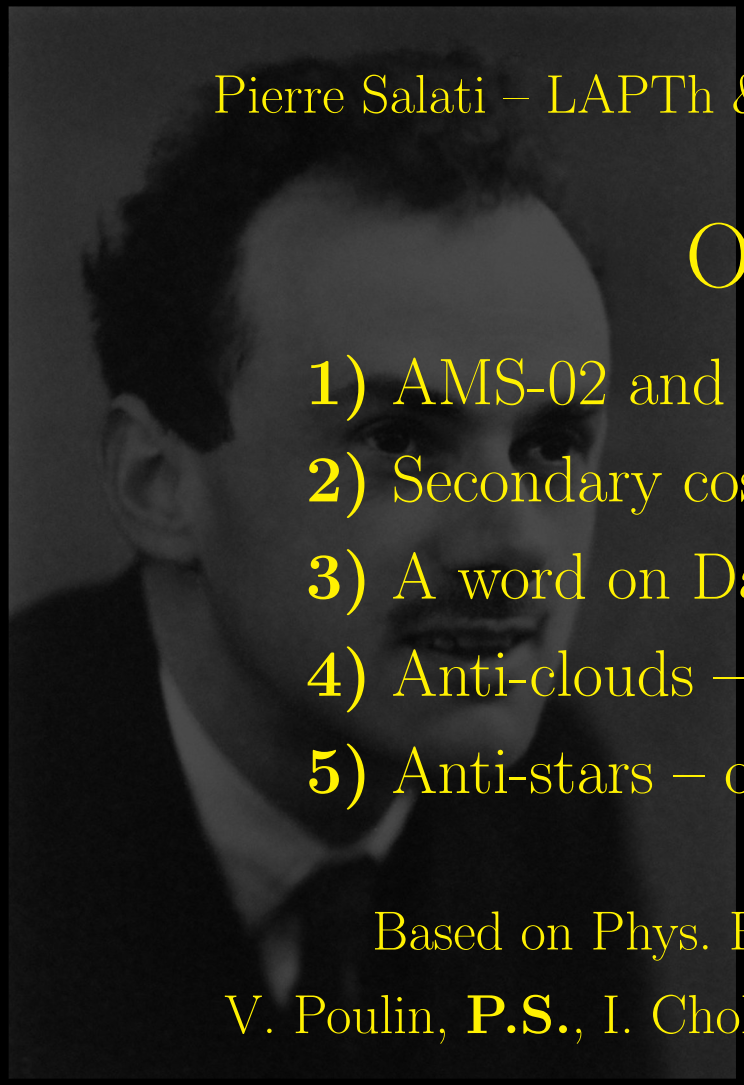

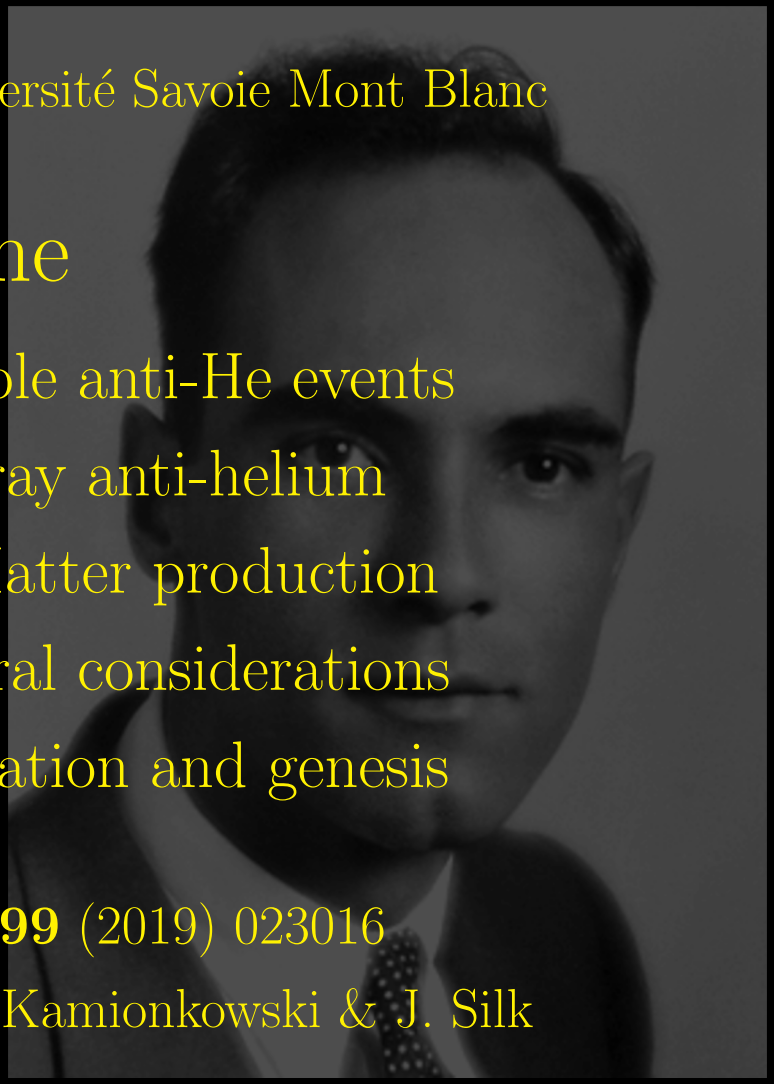

Outline

1) AMS-02 and possible anti-He events

2) Secondary cosmic-ray anti-helium

3) A word on Dark Matter production

4) Anti-clouds – general considerations

5) Anti-stars – observation and genesis

Based on Phys. Rev. **D99** (2019) 023016

V. Poulin, **P.S.**, I. Cholis, M. Kamionkowski & J. Silk

Corfu Summer Institute – Standard Model and Beyond – August 30, 2022

1) AMS-02 and possible anti-He events

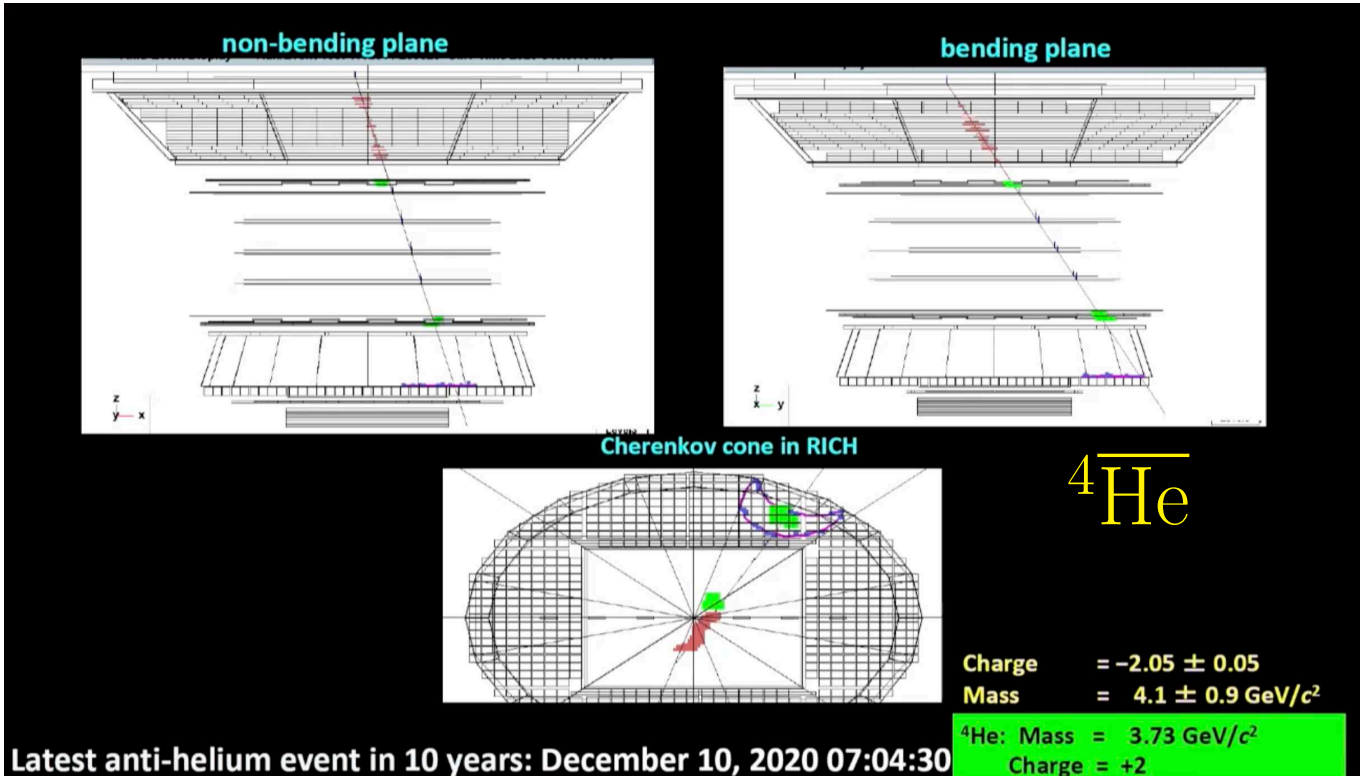

V. Choutko, Cosmic Heavy Anti-Matter, COSPAR E1.3-05-22, July 17th 2022

• AMS-02 has observed few events in the mass region from 0 to 10 GeV with charge $Z = -2$ and rigidity $\mathcal{R} < 50$ GV. The masses of all events are in the $^3\overline{\mathrm{He}}$ and $^4\overline{\mathrm{He}}$ mass region. As of 2018, 6 events $^3\overline{\mathrm{He}}$ and 2 events $^4\overline{\mathrm{He}}$.

• The event rate is 1 anti-helium in $\sim$ 100 million helium.

• Massive MC background simulations are carried out to evaluate significance. So far 35 billion He events simulated vs 6.8 billion He event triggers for 10 years. AMS-02 did not find background to the anti-helium events. At this level, the MC simulations are difficult to validate.

2) Secondary cosmic-ray anti-helium

$$q_{\rm sec}(\overline{\rm He}\,|\,E_{\overline{\rm He}},\boldsymbol{x}) = \sum_{i\in{\rm p},\alpha}\sum_{j\in{\rm H,He}} 4\,\pi \int dE_i\;\Phi_i(E_i,\boldsymbol{x})\,n_j(\boldsymbol{x})\,\frac{d\sigma_{ij\to\overline{\rm He}}}{dE_{\overline{\rm He}}}(E_i,E_{\overline{\rm He}})$$

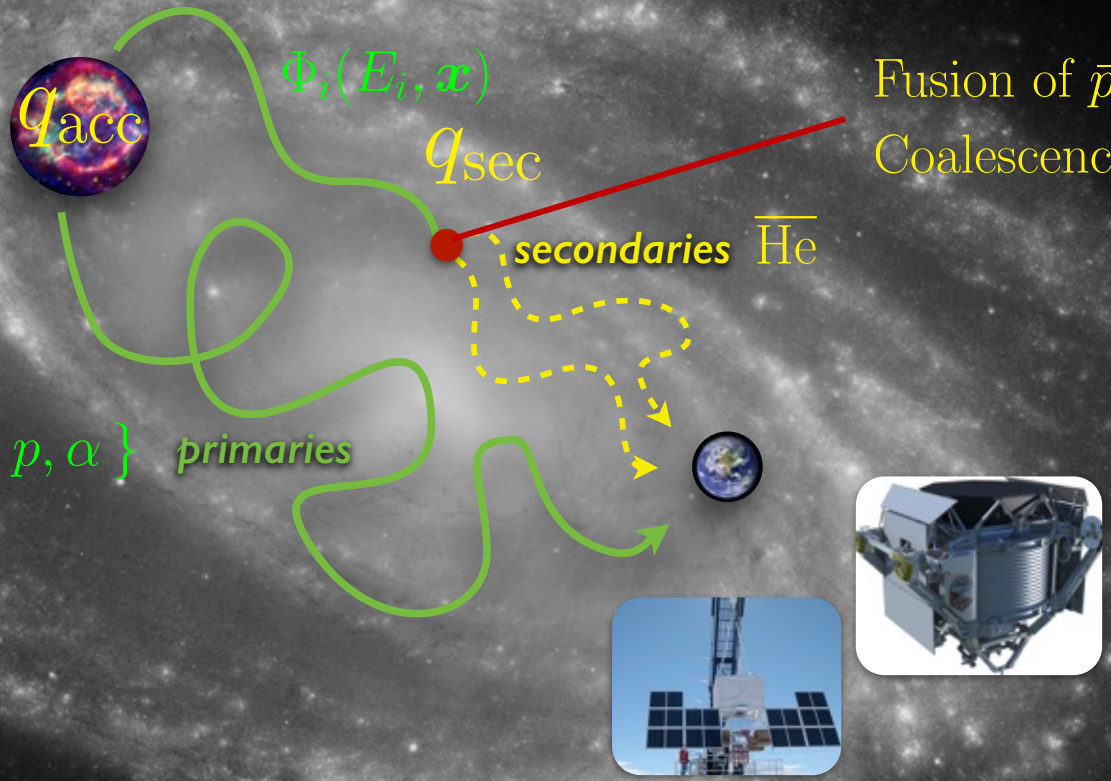

Fusion of $\bar{p}$ & $\bar{n}$
Coalescence factor B

Solar modulation with $\phi_p^{\rm F} \neq \phi_{\bar{p}}^{\rm F}$

Courtesy Antje Putze, TeVPA 2015

Anti-helium production and the coalescence factor

coalescence $\equiv$ fusion of $\bar{p}$ & $\bar{n}$ into $\bar{d}$, $\overline{^3\mathrm{He}}$ or $\overline{^4\mathrm{He}}$

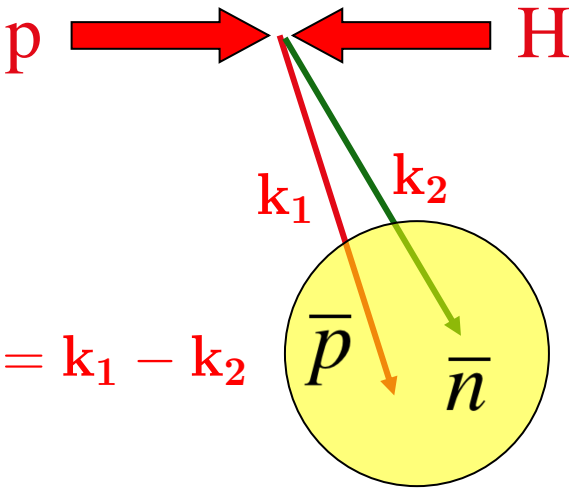

$2\boldsymbol{\Delta} = \mathbf{k_1} - \mathbf{k_2}$ $\qquad ||\boldsymbol{\Delta}|| \leq p_0$

coalescence momentum $p_0 = p_{\mathrm{coal}}/2$

$$d^3\mathcal{N}_{\bar{d}}(\mathbf{K}) = \int d^6\mathcal{N}_{\bar{p},\bar{n}}\,\{\mathbf{k_1},\mathbf{k_2}\} \times \mathcal{C}(\boldsymbol{\Delta}) \times \delta^3(\mathbf{K} - \mathbf{k_1} - \mathbf{k_2})$$

$$B_2 = \frac{E_{\bar{d}}}{E_{\bar{p}}\,E_{\bar{n}}} \int d^3\boldsymbol{\Delta}\; \mathcal{C}(\boldsymbol{\Delta}) \simeq \frac{m_{\bar{d}}}{m_{\bar{p}}\,m_{\bar{n}}} \left\{ \frac{4}{3}\pi\, p_0^3 \equiv \frac{\pi}{6}\, p_{\mathrm{coal}}^3 \right\}$$

Coalescence factor B_2

$$\frac{E_{\bar{d}}}{\sigma_{\mathrm{in}}} \frac{d^3\sigma_{\bar{d}}}{d^3\mathbf{K}} = B_2 \left\{ \frac{E_{\bar{p}}}{\sigma_{\mathrm{in}}} \frac{d^3\sigma_{\bar{p}}}{d^3\mathbf{k_1}} \right\} \left\{ \frac{E_{\bar{n}}}{\sigma_{\mathrm{in}}} \frac{d^3\sigma_{\bar{n}}}{d^3\mathbf{k_2}} \right\}$$

Anti-helium production and the coalescence factor

coalescence $\equiv$ fusion of $\bar{p}$ & $\bar{n}$ into $\bar{d}$, $\overline{^3\mathrm{He}}$ or $\overline{^4\mathrm{He}}$

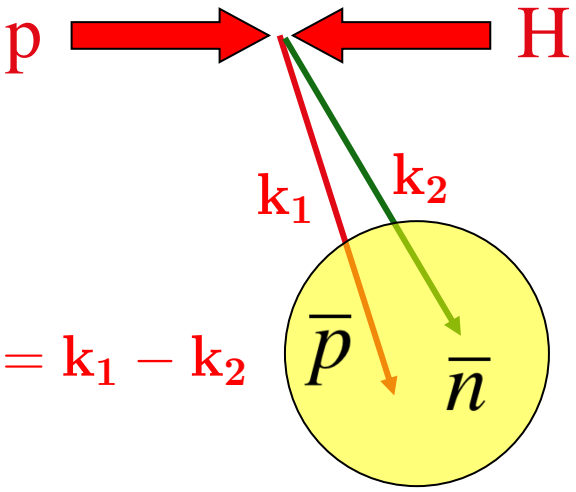

$2\boldsymbol{\Delta} = \mathbf{k_1} - \mathbf{k_2}$ $\qquad ||\boldsymbol{\Delta}|| \leq p_0$

coalescence momentum $p_0 = p_{\mathrm{coal}}/2$

Production on anti-nuclei with mass A

$$\frac{E_{\bar{A}}}{\sigma_{\mathrm{in}}}\frac{d^3\sigma_{\bar{A}}}{d^3\boldsymbol{k}_{\bar{A}}} = B_A \left\{\frac{E_{\bar{p}}}{\sigma_{\mathrm{in}}}\frac{d^3\sigma_{\bar{p}}}{d^3\boldsymbol{k}_{\bar{p}}}\right\}^Z \left\{\frac{E_{\bar{n}}}{\sigma_{\mathrm{in}}}\frac{d^3\sigma_{\bar{n}}}{d^3\boldsymbol{k}_{\bar{n}}}\right\}^{A-Z} \quad \text{with} \quad \boldsymbol{k}_{\bar{p}} = \boldsymbol{k}_{\bar{n}} = \boldsymbol{k}_{\bar{A}}/A$$

Coalescence factor B_A

$$B_A = \frac{m_A}{m_p^Z m_n^{A-Z}} \left\{\frac{\pi}{6} p_{\mathrm{coal}}^3\right\}^{A-1}$$

Determination of the coalescence momentum

- ALICE provides an **experimental** determination of B_2 and B_3.
  $\bar{p}$ production cross-section is **measured**.
  Approximately the same value for p_0 from $\bar{d}$, $\bar{t}$ and $^3\overline{\mathrm{He}}$.

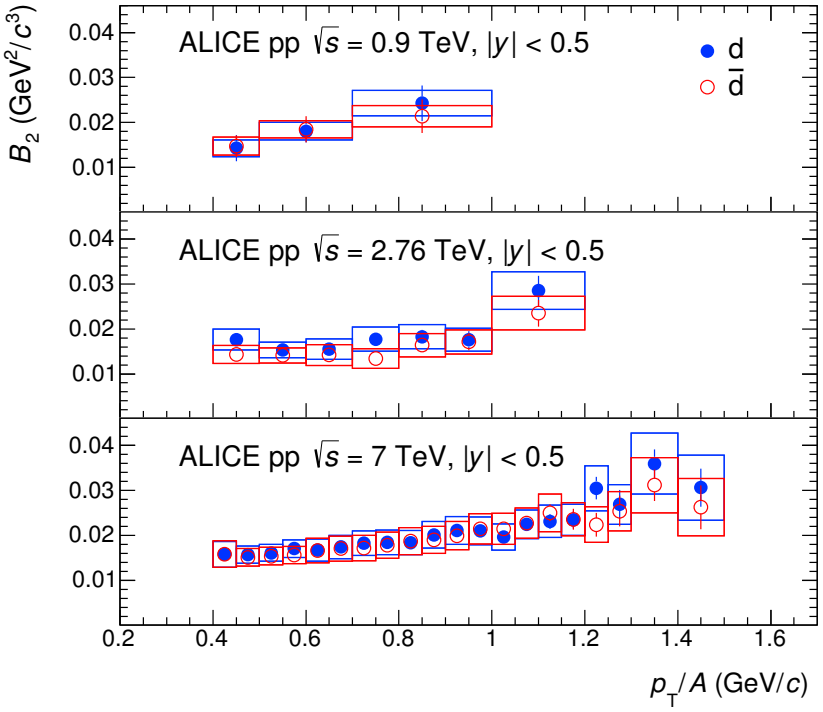

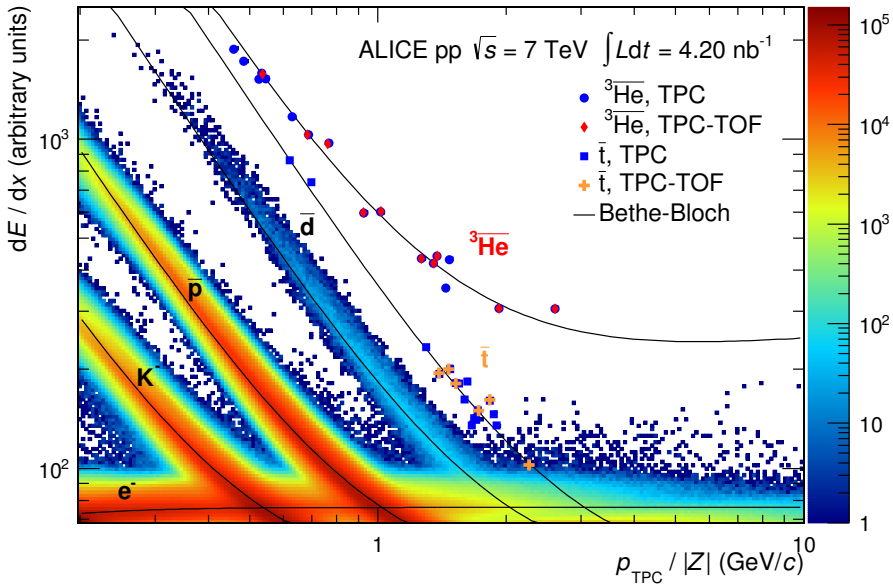

S. Acharya et al., Phys. Rev. **C97** (2018) 024615

Determination of the coalescence momentum

- ALICE provides an **experimental** determination of B_2 and B_3.
  $\bar{p}$ production cross-section is **measured**.
  Approximately the same value for p_0 from $\bar{d}$, $\bar{t}$ and $^3\overline{\mathrm{He}}$.

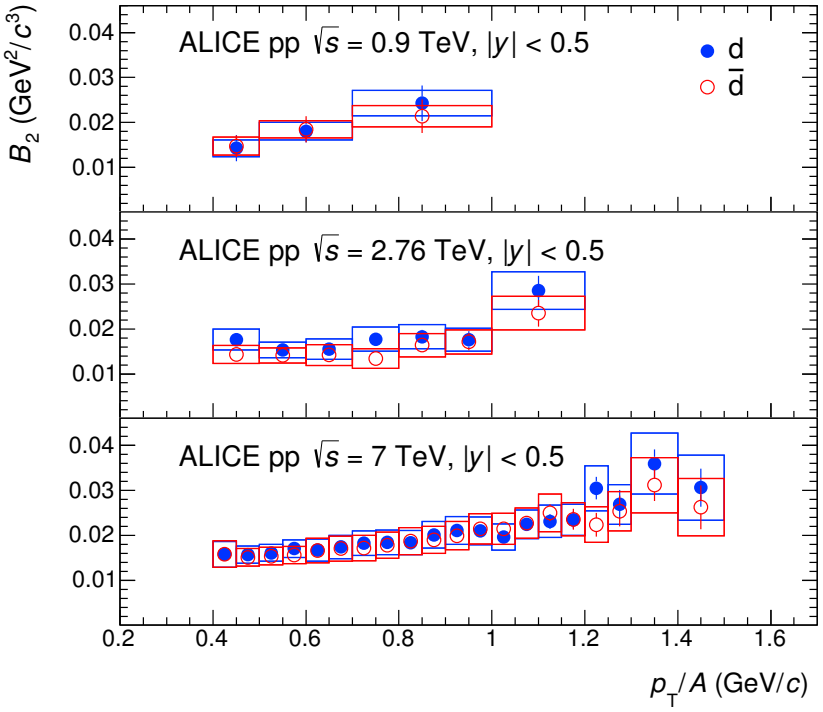

208 MeV $\leq p_{\mathrm{coal}} \leq$ 262 MeV

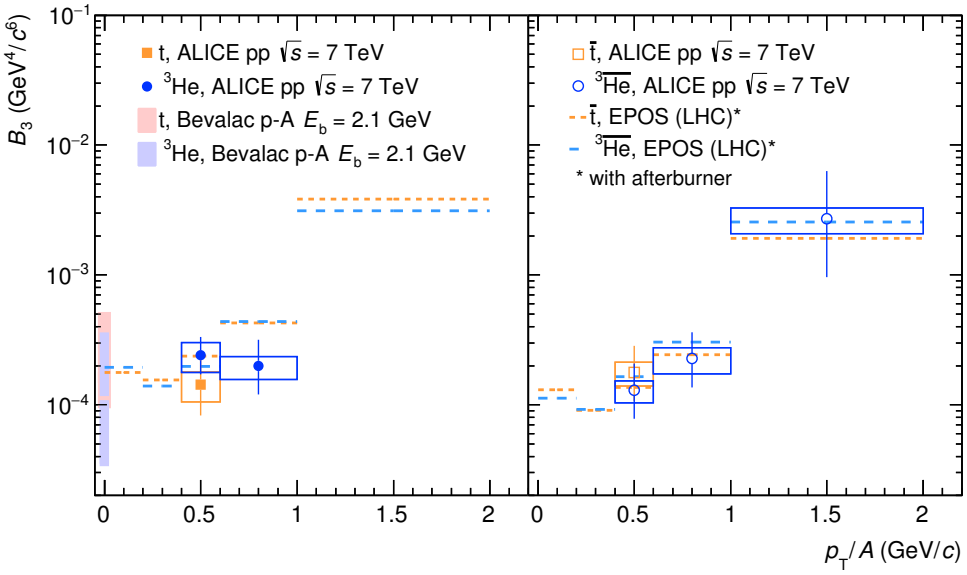

218 MeV $\leq p_{\mathrm{coal}} \leq$ 262 MeV

S. Acharya et al., Phys. Rev. **C97** (2018) 024615

Local source term for anti-nuclei production in cosmic-rays

$$q_{\rm sec}(\overline{\rm He}\,|\,E_{\overline{\rm He}},\boldsymbol{x}) = \sum_{i\in{\rm p},\alpha}\sum_{j\in{\rm H,He}} 4\,\pi \int dE_i\;\Phi_i(E_i,\boldsymbol{x})\,n_j(\boldsymbol{x})\,\frac{d\sigma_{ij\to\overline{\rm He}}}{dE_{\overline{\rm He}}}(E_i,E_{\overline{\rm He}})$$

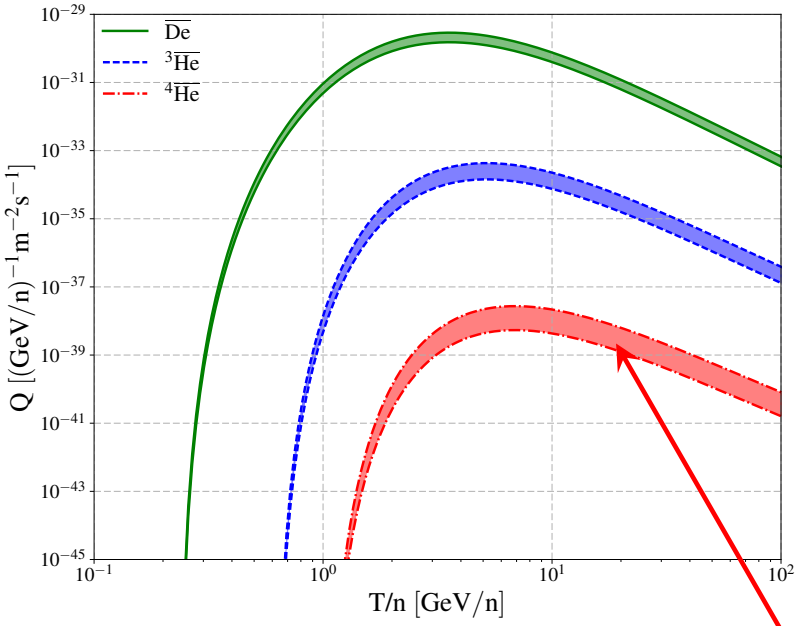

V. Poulin et al., Phys. Rev. **D99** (2019) 023016

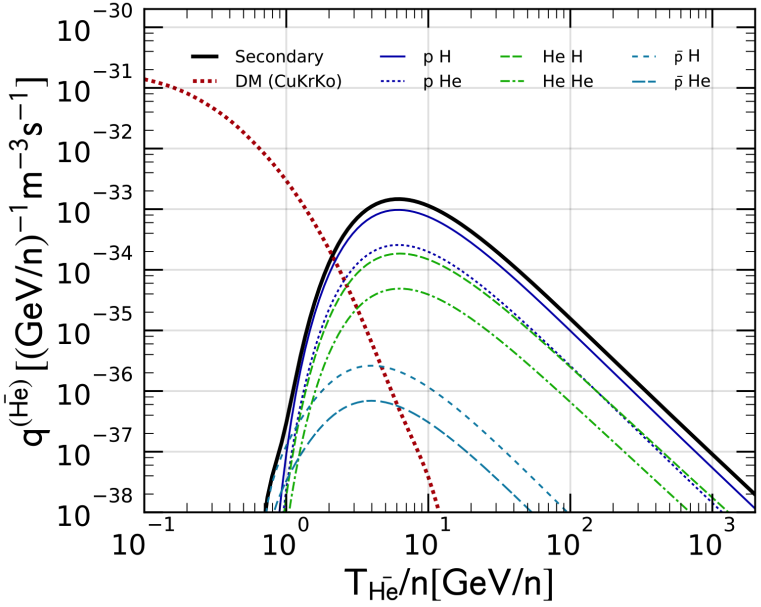

M. Korsmeier et al., Phys. Rev. **D97** (2018) 103011

$$7.7\times10^{-7} \le \frac{B_4}{\rm GeV^6} \le 3.9\times10^{-6}$$

$\bar{p}$ production modeled as in
M. di Mauro et al., Phys. Rev. **D90** (2014) 085017

Charged cosmic-ray Galactic propagation

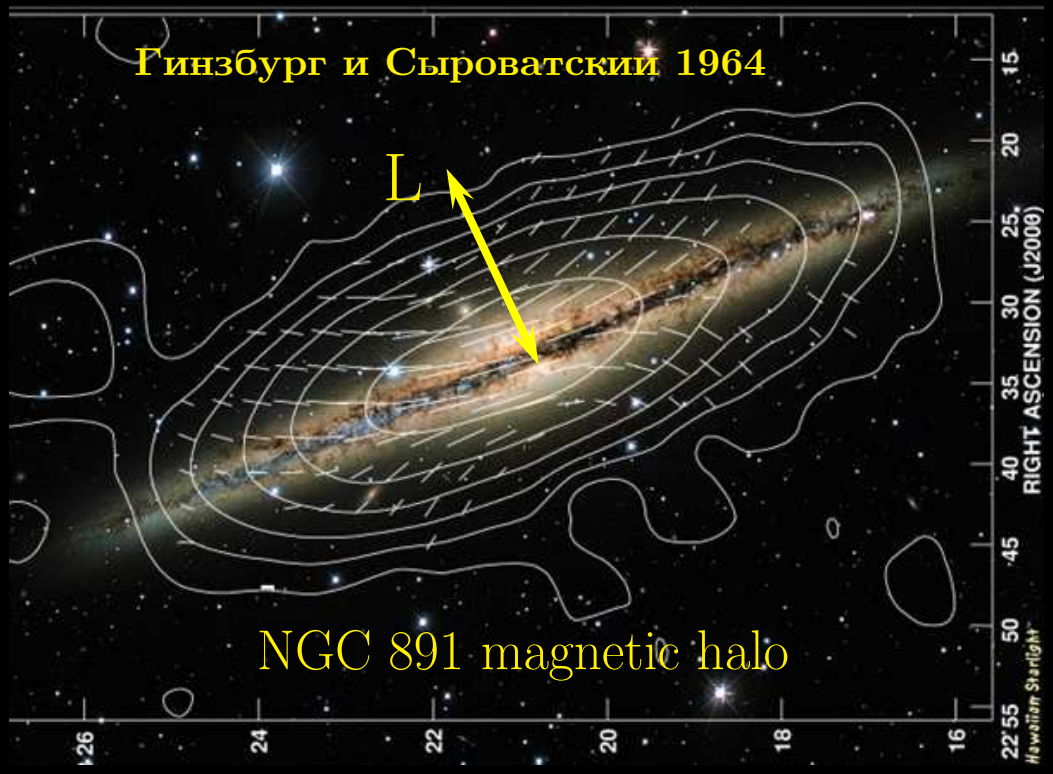

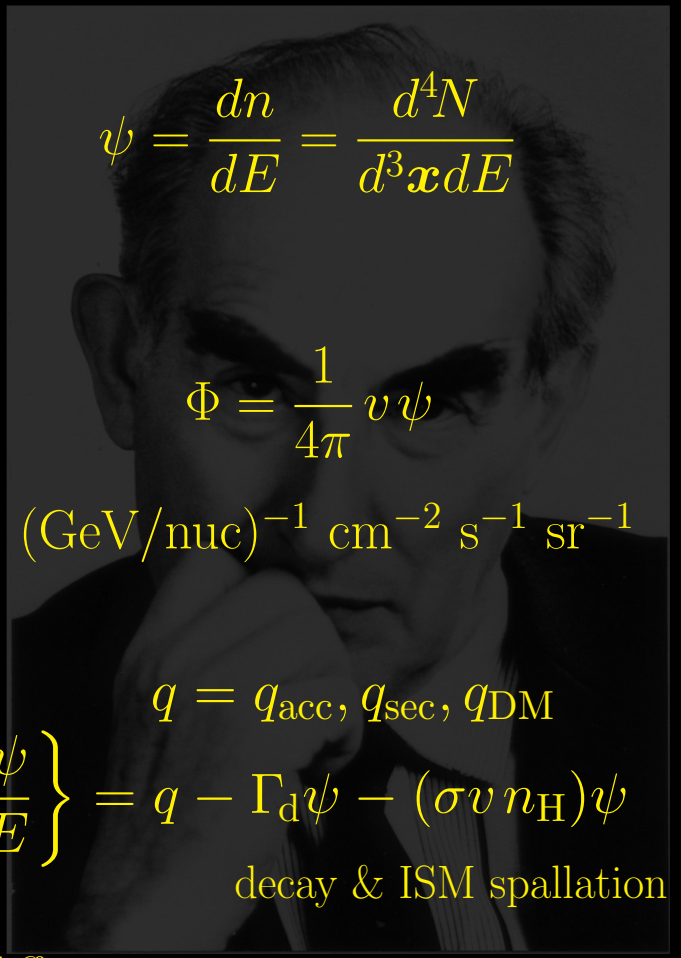

$$\psi = \frac{dn}{dE} = \frac{d^4N}{d^3\boldsymbol{x}dE}$$

$$\Phi = \frac{1}{4\pi} v\psi$$

$$(\mathrm{GeV/nuc})^{-1}\ \mathrm{cm}^{-2}\ \mathrm{s}^{-1}\ \mathrm{sr}^{-1}$$

$$q = q_{\rm acc}, q_{\rm sec}, q_{\rm DM}$$

$$\dot{\psi} + \boldsymbol{\nabla}\cdot\{-K\boldsymbol{\nabla}\psi + \psi\boldsymbol{V}_C\} + \frac{\partial}{\partial E}\left\{b\psi - D_{EE}\frac{\partial\psi}{\partial E}\right\} = q - \Gamma_{\rm d}\psi - (\sigma v\, n_{\rm H})\psi$$

convection — E losses — decay & ISM spallation

$\boldsymbol{x}$ diffusion — E diffusion

$$K = \beta^\eta K_0 \left\{1 + \left(\frac{R_{\rm l}}{R}\right)^{\frac{\delta-\delta_{\rm l}}{s_{\rm l}}}\right\}^{s_{\rm l}} \left(\frac{R}{1\,\mathrm{GV}}\right)^{\delta} \left\{1 + \left(\frac{R}{R_{\rm h}}\right)^{\frac{\delta-\delta_{\rm h}}{s_{\rm h}}}\right\}^{-s_{\rm h}}$$

$$D_{EE} = \frac{4}{3}\frac{\beta^2}{\delta(4-\delta^2)(4-\delta)}\frac{V_a{}^2 p^2}{K}$$

Secondary anti-helium fluxes

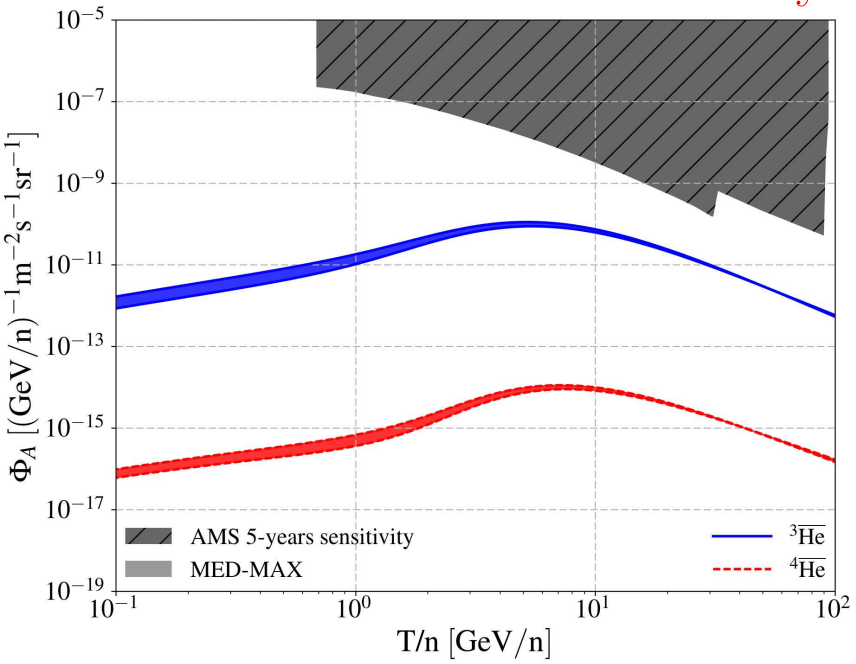

V. Poulin et al., Phys. Rev. **D99** (2019) 023016

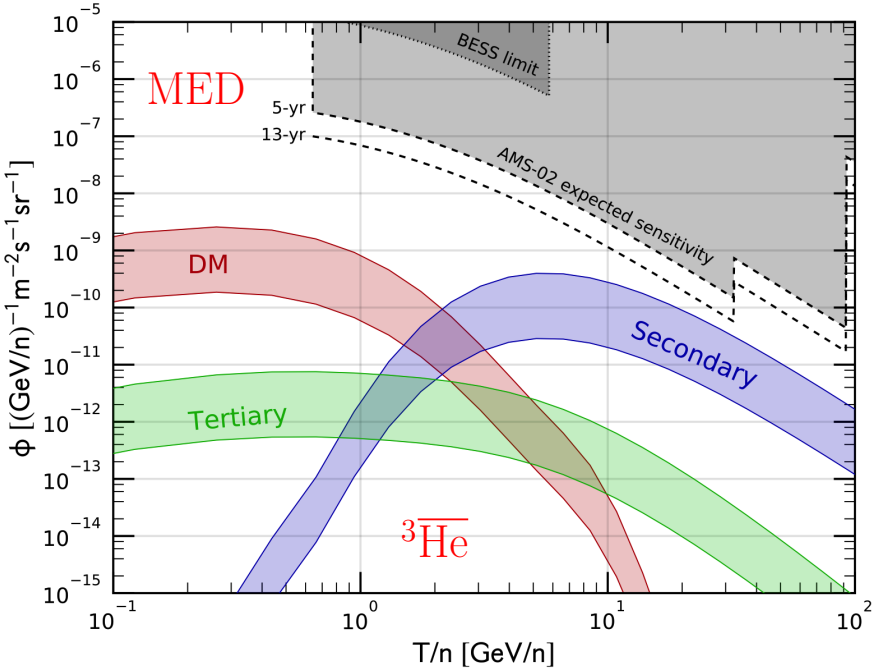

M. Korsmeier et al., Phys. Rev. **D97** (2018) 103011

- Interactions of high-energy cosmic-ray protons and helium nuclei on the ISM yield a **secondary anti-He flux** well below AMS-02 sensitivity.
- The same conclusion holds for DM decays or annihilations although M. Winkler and T. Linden have proposed a nice counter-example based on $\bar{\Lambda}_b$ production if pure $^3\overline{\mathrm{He}}$ events – Winkler+[2006.16251].
- The General Antiparticle Spectrometer (GAPS) is about to fly and measure the $\bar{p}$ flux below 200 MeV. GAPS has a cute way to disentangle $\bar{p}$ from $\bar{d}$.
- Dark Matter has triggered a hectic activity and has been systematicaly hunted for. It may be time now to devote some attention to the possibility of anti-matter domains in the universe – **anti-clouds & anti-stars**.

3) A word on Dark Matter production

- In general, DM species annihilations do not produce a detectable amount of antihelium nuclei $^3\overline{\text{He}}$.
- Since DM is at rest, the spectrum peaks at low energy $\neq \mathcal{O}(10)$ GeV/n.
- Recently, a new proposal based on DM coupling to b quarks.

$$\chi + \chi \to b + \bar{b} \qquad \bar{b} \to \bar{\Lambda}_b \text{ meson } (\bar{b}\bar{u}\bar{d})$$

$$\bar{\Lambda}_b\,(5.6\ \text{GeV}) \to \overline{^3\text{He}} + 2p\,(4.7\ \text{GeV})$$

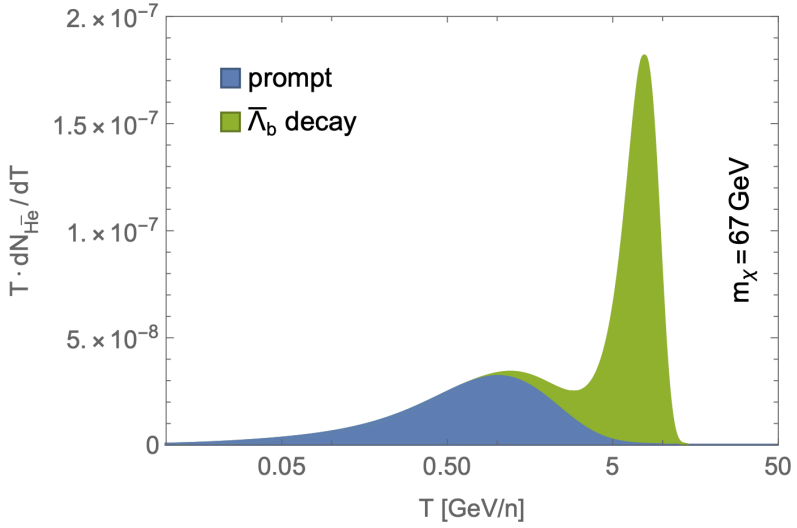

experiment	channel	measurement	Pythia (default)	Pythia (Λ_b-tune)
LEP [4, 5]	$f(b \to \Lambda_b)$	$0.101^{+0.039}_{-0.031}$	0.037	0.101
LEP [6]	$f(b \to \Lambda_b, \Xi_b, \Omega_b)$	0.117 ± 0.021	0.047	0.127
Tevatron CDF [7]	$\frac{f(b\to\Lambda_b)}{f(b\to B)}$	$0.281^{+0.141}_{-0.103}$	0.046	0.135
LHCb [8]	$\frac{f(b\to\Lambda_b)}{f(b\to B)}$	0.259 ± 0.018	0.048	0.134

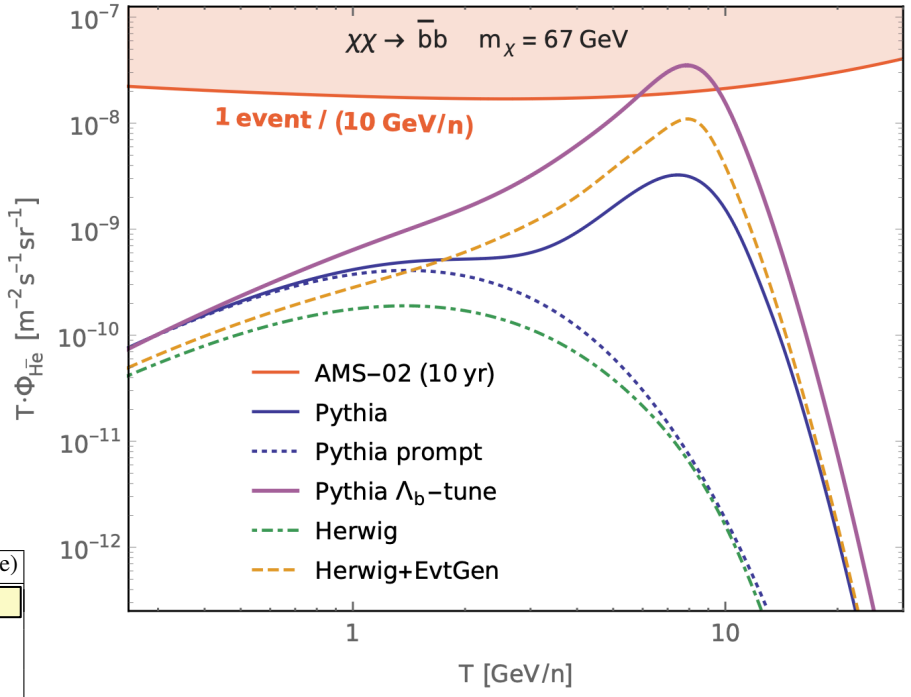

Winkler+[2006.16251]

Counterarguments – Kachelriess+[2105.00799]

• To get the value of $f(b \to \Lambda_b)$ measured at LEP, WL21 have increased the probability `probQQtoQ` for diquark formation in hadronization from 0.09 to 0.24, playing havoc with other processes.

• This implies:
(i) an over production of protons and antiprotons at LEP by a factor of 2,
(ii) an increase in proton yield with respect to kaon and pion yields $dN/dy|_{|y|<0.5}$ measured by ALICE at LHC.

• In default Pythia, $\mathrm{Br}(\bar{\Lambda}_b \to \overline{^3\mathrm{He}}) \simeq 3 \times 10^{-6}$ may already be too large. Default Pythia overestimates branching ratios for several Λ_b decay channels. Mismodeling of diquark formation.

$\sqrt{s}$	≈ 10 GeV	29–35 GeV	91 GeV	130–200 GeV
Obs.	0.266 ± 0.008	0.640 ± 0.050	1.050 ± 0.032	1.41 ± 0.18
WL21	0.640	1.161	2.102	2.33

p and $\bar{p}$ multiplicity in e^+e^- annihilations

Particle	proton	kaon	pion
$\mathrm{d}N/\mathrm{d}y$, LHC	0.124 ± 0.009	0.286 ± 0.016	2.26 ± 0.10
$\mathrm{d}N/\mathrm{d}y$, Λ_b tune	0.328	0.231	1.90

dN/dy at mid-rapidity $|y| < 0.5$
at LHC at $\sqrt{s} = 7$ TeV for p, K^+ and π^+

Branching ratio	PDG	Pythia
$\Lambda_b \to \Lambda_c^+ p\bar{p}\pi^-$	2.65×10^{-4}	1.5×10^{-3}
$\Lambda_b \to \Lambda_c^+ \pi^+\pi^-\pi^-$	7.7×10^{-3}	0.047
$\Lambda_b \to \Lambda\pi^+\pi^-$	4.7×10^{-6}	2.0×10^{-5}
$\Lambda_b \to p\pi^-\pi^+\pi^-$	2.11×10^{-5}	9.6×10^{-5}
$\Lambda_b \to pK^-K^+\pi^-$	4.1×10^{-6}	1.7×10^{-5}
$B^0 \to p\bar{p}K^0$	2.66×10^{-6}	6.1×10^{-6}
$B^0 \to p\bar{p}\pi^+\pi^-$	2.87×10^{-6}	5.6×10^{-6}
$B^0 \to \Lambda_c^- p\pi^+\pi^-$	1.02×10^{-3}	2.1×10^{-3}
$\Lambda_c \to p\pi^+\pi^-$	4.61×10^{-3}	0.012
$\Lambda_c \to p\pi^0$	$< 2.7 \times 10^{-4}$	2.0×10^{-3}
$\Lambda_c \to \Lambda K^+\pi^+\pi^-$	$< 5 \times 10^{-4}$	2.1×10^{-3}

Let us measure $\mathrm{Br}(\bar{\Lambda}_b \to \overline{^3\mathrm{He}})$ and see!

4) Anti-clouds – general considerations

Domains of anti-matter gas inside the Milky Way disk and in the early universe

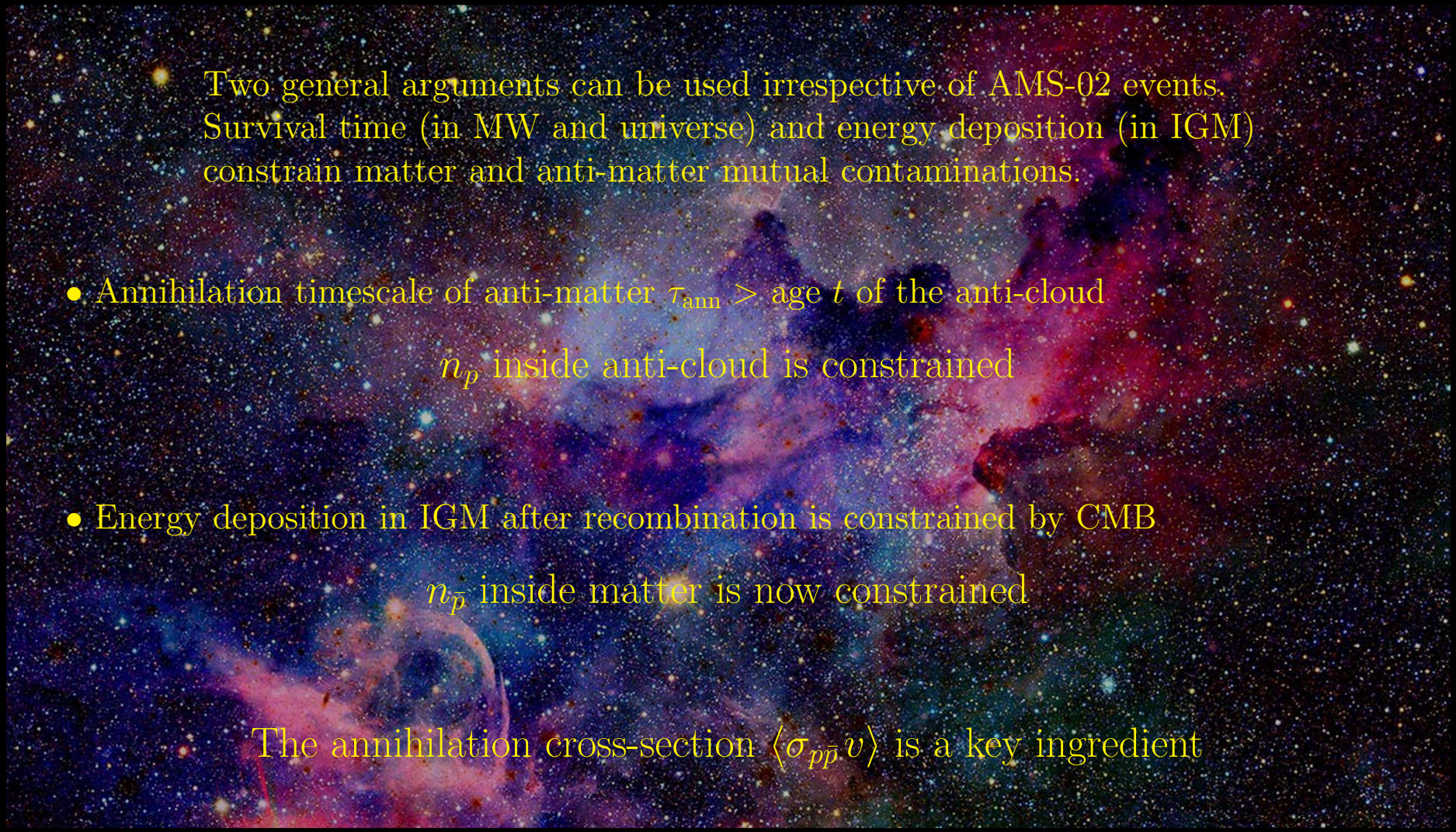

Two general arguments can be used irrespective of AMS-02 events.
Survival time (in MW and universe) and energy deposition (in IGM) constrain matter and anti-matter mutual contaminations.

- Annihilation timescale of anti-matter $\tau_{\rm ann} >$ age t of the anti-cloud

n_p inside anti-cloud is constrained

- Energy deposition in IGM after recombination is constrained by CMB

$n_{\bar{p}}$ inside matter is now constrained

The annihilation cross-section $\langle \sigma_{p\bar{p}} v \rangle$ is a key ingredient

proton-antiproton annihilation cross-section $\langle \sigma_{p\bar{p}} v \rangle$

$\langle \sigma_{p\bar{p}} v \rangle$

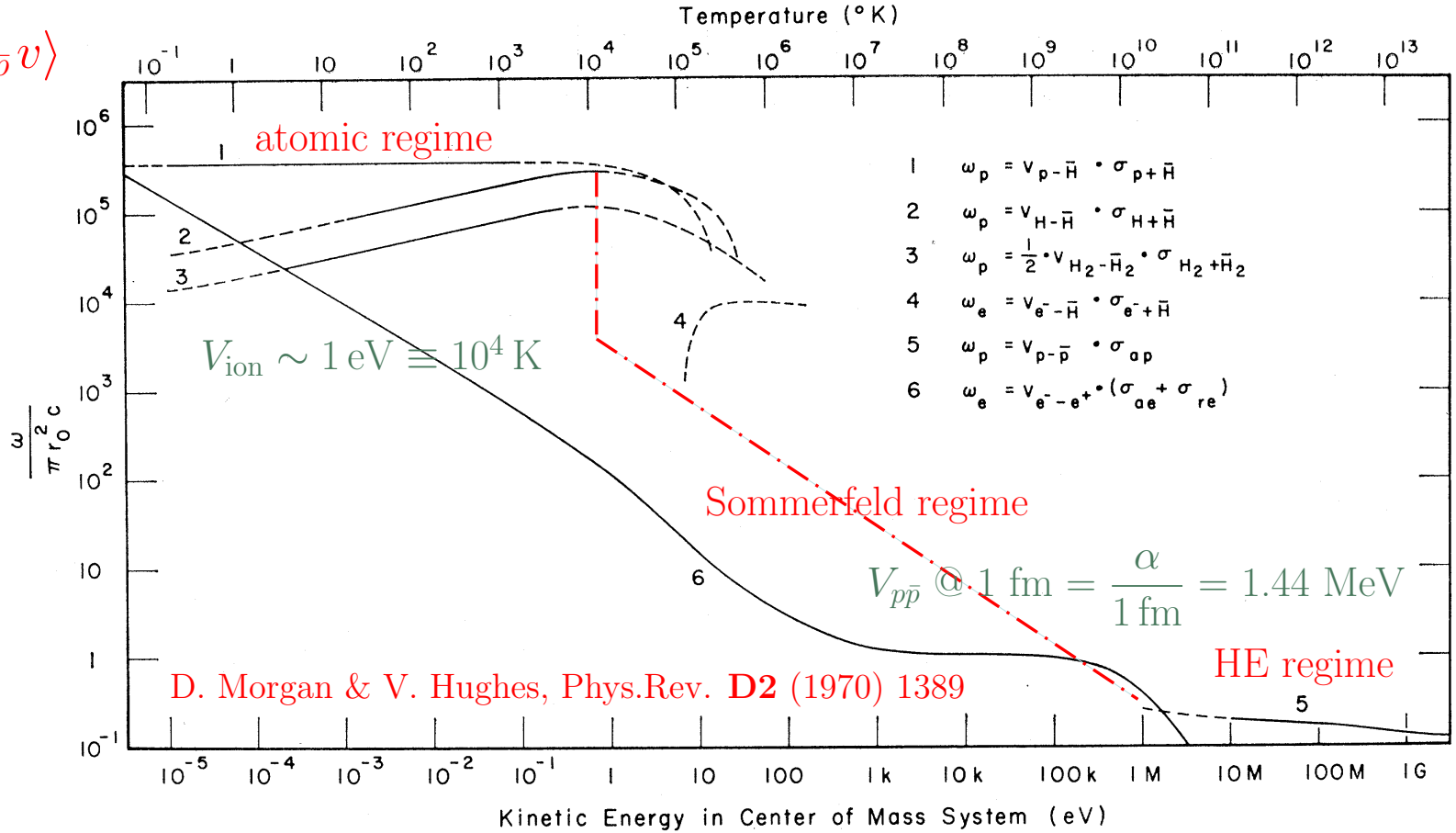

FIG. 4. Per particle per unit antiparticle number-density annihilation rates for various processes producing annihilation. The approximate temperature is shown.

$$\langle \sigma_{p\bar{p}} v \rangle \simeq \begin{cases} 1.5 \times 10^{-15}\ {\rm cm}^3/{\rm s} & T > 10^{10}\ {\rm K} \\ 10^{-10} \left(\frac{\rm K}{T}\right)^{1/2}\ {\rm cm}^3/{\rm s} & 10^{10}\ {\rm K} > T > 10^4\ {\rm K} \\ 10^{-10}\ {\rm cm}^3/{\rm s} & 10^4\ {\rm K} > T \end{cases}$$

G. Steigman, Ann. Rev. Astron. Astrophys. **14** (1976) 339

Anti-clouds in the disk of the Milky Way (MW)

Anti-matter should survive annihilation, hence a very small density of matter inside anti-matter clouds. The survival rate depends on whether anti-matter is in the form of cold clouds, where $T \sim \mathcal{O}(30)$ K, or in hot ionized clouds, where $T \sim \mathcal{O}(10^6)$ K.

$$\tau_{\rm ann} = \frac{1}{\langle \sigma_{p\bar{p}} v \rangle n_p} > t_{\rm MW} \simeq 9 \times 10^9 \, {\rm y}$$

$$\Downarrow$$

$$n_p^{\rm cold} < 3.5 \times 10^{-8} \, {\rm cm}^{-3} \quad \text{while} \quad n_p^{\rm hot} < 3.5 \times 10^{-5} \, {\rm cm}^{-3}$$

Structure of interstellar medium (ISM)

TABLE I. Descriptive parameters of the different components of the interstellar gas, according to the references quoted in the main text. T is the temperature, n is the true (as opposed to space-averaged) number density of hydrogen nuclei near the Sun, $\Sigma_\odot$ is the azimuthally-averaged mass density per unit area at the solar circle, and $\mathcal{M}$ is the mass contained in the entire Milky Way. Both $\Sigma_\odot$ and $\mathcal{M}$ include 70.4 % of hydrogen, 28.1 % of helium, and 1.5 % of heavier elements. All values were rescaled to $R_\odot = 8.5$ kpc, in accordance with footnote 3.

Component	T (K)	n (cm^{-3})	$\Sigma_\odot$ ($M_\odot$ pc^{-2})	$\mathcal{M}$ (10^9 $M_\odot$)
Molecular	$10 - 20$	$10^2 - 10^6$	~ 2.5	$\sim 1.3^{\rm a} - 2.5^{\rm b}$
Cold atomic	$50 - 100$	$20 - 50$	~ 3.5	$\gtrsim 6.0$
Warm atomic	$6000 - 10000$	$0.2 - 0.5$	~ 3.5	
Warm ionized	~ 8000	$0.2 - 0.5$	~ 1.4	$\gtrsim 1.6$
Hot ionized	$\sim 10^6$	~ 0.0065		

[a] adapted from Bronfman *et al.*, 1988.
[b] adapted from Clemens *et al.*, 1988.

K.M. Ferriere, Rev. Mod. Phys. **73** (2001) 1031

Anti-clouds in the disk of the Milky Way (MW)

Anti-matter should survive annihilation, hence a very small density of matter inside anti-matter clouds. The survival rate depends on whether anti-matter is in the form of cold clouds, where $T \sim \mathcal{O}(30)$ K, or in hot ionized clouds, where $T \sim \mathcal{O}(10^6)$ K.

$$\tau_{\rm ann} = \frac{1}{\langle \sigma_{p\bar{p}} v \rangle n_p} > t_{\rm MW} \simeq 9 \times 10^9 \, {\rm y}$$

$$\Downarrow$$

$$n_p^{\rm cold} < 3.5 \times 10^{-8} \, {\rm cm}^{-3} \quad \text{while} \quad n_p^{\rm hot} < 3.5 \times 10^{-5} \, {\rm cm}^{-3}$$

Structure of interstellar medium (ISM)

TABLE I. Descriptive parameters of the different components of the interstellar gas, according to the references quoted in the main text. T is the temperature, n is the true (as opposed to space-averaged) number density of hydrogen nuclei near the Sun, $\Sigma_\odot$ is the azimuthally-averaged mass density per unit area at the solar circle, and $\mathcal{M}$ is the mass contained in the entire Milky Way. Both $\Sigma_\odot$ and $\mathcal{M}$ include 70.4 % of hydrogen, 28.1 % of helium, and 1.5 % of heavier elements. All values were rescaled to $R_\odot = 8.5$ kpc, in accordance with footnote 3.

Component	T (K)	n (cm^{-3})	$\Sigma_\odot$ ($M_\odot$ pc^{-2})	$\mathcal{M}$ (10^9 $M_\odot$)
Molecular	$10 - 20$	$10^2 - 10^6$	~ 2.5	$\sim 1.3^{\rm a} - 2.5^{\rm b}$
Cold atomic	$50 - 100$	$20 - 50$	~ 3.5	$\gtrsim 6.0$
Warm atomic	$6000 - 10000$	$0.2 - 0.5$	~ 3.5	
Warm ionized	~ 8000	$0.2 - 0.5$	~ 1.4	$\gtrsim 1.6$
Hot ionized	$\sim 10^6$	~ 0.0065		

[a] adapted from Bronfman *et al.*, 1988.
[b] adapted from Clemens *et al.*, 1988.

K.M. Ferriere, Rev. Mod. Phys. **73** (2001) 1031

Segregation factor between 10^{-14} (cold) and 0.005 (hot)

Anti-clouds surviving in the early universe

The same calculation can be performed in the early universe, splitting between three periods depending on the annihilation regime. The annihilation timescale needs to be compared to the age of the universe at **redshift** z.

$$\tau_{\rm ann} = \frac{1}{\langle \sigma_{p\bar{p}} v \rangle n_p} > t_{\rm U} \simeq \begin{cases} 10^{19}\,{\rm s}\,(1+z)^{-2} & \text{radiation} \\ 3\times 10^{17}\,{\rm s}\,(1+z)^{-3/2} & \text{matter} \end{cases}$$

$$\Downarrow$$

Constraint on $n_p^{\rm local}/n_p^{\rm cosmo}$ where $n_p^{\rm cosmo} = 2.534\times 10^{-7}\,(1+z)^3\,{\rm cm}^{-3}$

$$\Downarrow$$

- Before BBN era $T > 10^{10}\,{\rm K}$

$$n_p^{\rm local}/n_p^{\rm cosmo} \leq \frac{263}{(1+z)} \text{ with } z \geq 3.5\times 10^9$$

- After BBN and before matter-radiation equality, i.e. $10^4\,{\rm K} < T < 10^{10}\,{\rm K}$

$$n_p^{\rm local}/n_p^{\rm cosmo} \leq \frac{3.25\times 10^{-3}}{\sqrt{1+z}} \text{ with } 3.5\times 10^3 \leq z \leq 3.5\times 10^9$$

- During the matter domination era, i.e. $T < 10^4\,{\rm K}$

$$n_p^{\rm local}/n_p^{\rm cosmo} \leq \frac{0.13}{(1+z)^{3/2}} \text{ with } z \leq 3.5\times 10^3$$

Anti-clouds surviving in the early universe

The same calculation can be performed in the early universe, splitting between three periods depending on the annihilation regime. The annihilation timescale needs to be compared to the age of the universe at **redshift** z.

$$\tau_{\rm ann} = \frac{1}{\langle \sigma_{p\bar{p}} v \rangle n_p} > t_{\rm U} \simeq \begin{cases} 10^{19}\,{\rm s}\,(1+z)^{-2} & \text{radiation} \\ 3\times 10^{17}\,{\rm s}\,(1+z)^{-3/2} & \text{matter} \end{cases}$$

$$\Downarrow$$

Constraint on $n_p^{\rm local}/n_p^{\rm cosmo}$ where $n_p^{\rm cosmo} = 2.534\times 10^{-7}\,(1+z)^3\,{\rm cm}^{-3}$

Segregation factor between $\leq 7\times 10^{-8}$ (BBN) and 0.13 (now)

- Before BBN era $T > 10^{10}\,{\rm K}$

$$n_p^{\rm local}/n_p^{\rm cosmo} \leq \frac{263}{(1+z)} \text{ with } z \geq 3.5\times 10^9$$

- After BBN and before matter-radiation equality, i.e. $10^4\,{\rm K} < T < 10^{10}\,{\rm K}$

$$n_p^{\rm local}/n_p^{\rm cosmo} \leq \frac{3.25\times 10^{-3}}{\sqrt{1+z}} \text{ with } 3.5\times 10^3 \leq z \leq 3.5\times 10^9$$

- During the matter domination era, i.e. $T < 10^4\,{\rm K}$

$$n_p^{\rm local}/n_p^{\rm cosmo} \leq \frac{0.13}{(1+z)^{3/2}} \text{ with } z \leq 3.5\times 10^3$$

Energy injection in the intergalatic medium

Energy injected after recombination modifies the re-ionization history of the IGM and its optical depth against Thomson scattering. It eventually modifies polarization anisotropies in the CMB, hence strong contraints from Planck.

$$\left.\frac{\mathrm{d}^2 E}{\mathrm{d}V\,\mathrm{d}t}\right|_{\mathrm{DM}} = \tfrac{1}{2}\langle\sigma_{\mathrm{ann}} v\rangle n_{\mathrm{DM}}^2 \times 2\, m_{\mathrm{DM}} c^2 \times f_{\mathrm{eff}}$$

$$\Downarrow$$

$$\left.\frac{\mathrm{d}^2 E}{\mathrm{d}V\,\mathrm{d}t}\right|_{\mathrm{DM}} = \left\{ p_{\mathrm{ann}} \equiv f_{\mathrm{eff}} \frac{\langle\sigma_{\mathrm{ann}} v\rangle}{m_{\mathrm{DM}}} \right\} \left\{ \rho_c^0\, \Omega_{\mathrm{CDM}}\, c \right\}^2 (1+z)^6$$

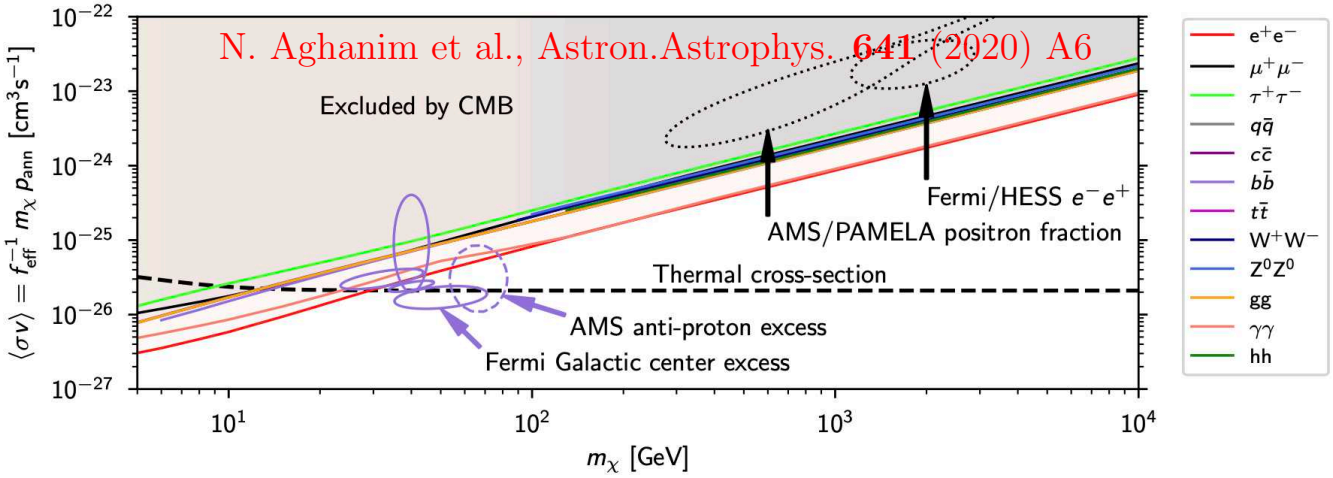

$$p_{\mathrm{ann}} \leq 3.2 \times 10^{-28}\,\mathrm{cm}^3\,\mathrm{s}^{-1}\,\mathrm{GeV}^{-1}$$

$$\Downarrow$$

$$\left.\frac{\mathrm{d}^2 E}{\mathrm{d}V\,\mathrm{d}t}\right|_{\mathrm{DM}} \leq 8.26 \times 10^{-44}\,(1+z)^6\,\mathrm{J\,m^{-3}\,s^{-1}}$$

Energy injection in the intergalatic medium

$$\left.\frac{\mathrm{d}^2 E}{\mathrm{d}V\,\mathrm{d}t}\right|_{\mathrm{DM}} = \langle\sigma_{p\bar{p}}v\rangle n_p n_{\bar{p}} \times 2\,m_p c^2 = \langle\sigma_{p\bar{p}}v\rangle n_p^0 n_{\bar{p}}^0 \times 2\,m_p c^2\,(1+z)^6$$

$$\Downarrow$$

$$n_{\bar{p}}^0 \leq 1.1 \times 10^{-23}\,\mathrm{cm}^{-3} \left\{\frac{10^{-10}\,\mathrm{cm}^3\,\mathrm{s}^{-1}}{\langle\sigma_{p\bar{p}}v\rangle}\right\}$$

4.3×10^{-17} smaller than $n_p^0 = 2.534 \times 10^{-7}\,\mathrm{cm}^{-3}$

$$\Uparrow$$

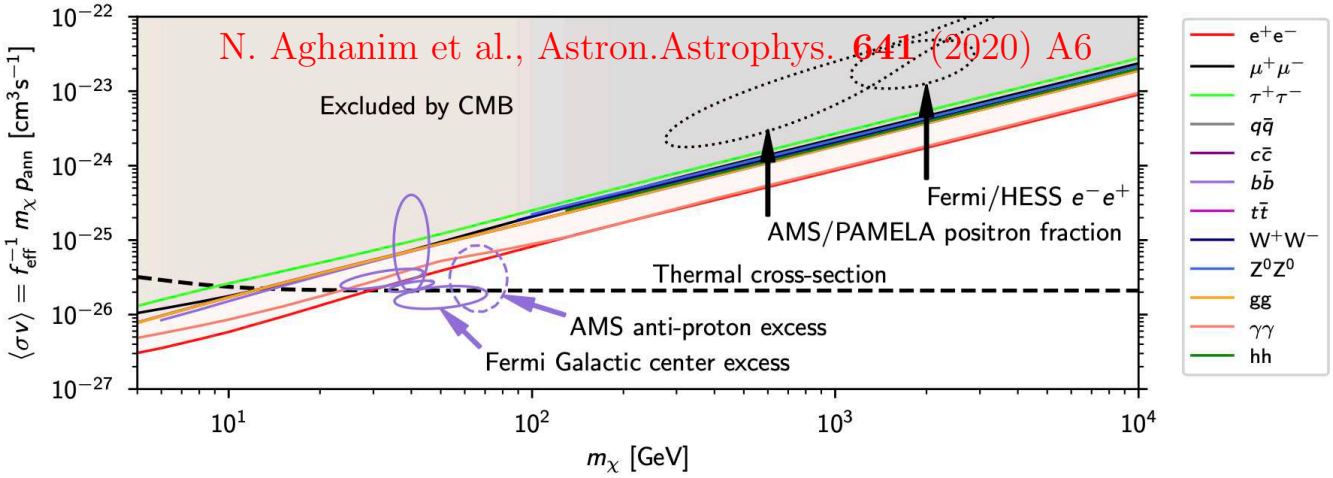

$$p_{\mathrm{ann}} \leq 3.2 \times 10^{-28}\,\mathrm{cm}^3\,\mathrm{s}^{-1}\,\mathrm{GeV}^{-1}$$

$$\Downarrow$$

$$\left.\frac{\mathrm{d}^2 E}{\mathrm{d}V\,\mathrm{d}t}\right|_{\mathrm{DM}} \leq 8.26 \times 10^{-44}\,(1+z)^6\,\mathrm{J}\,\mathrm{m}^{-3}\,\mathrm{s}^{-1}$$

5) Anti-stars – observation and genesis

Anti-matter could alternatively be in the form of anti-stars. They could essentially be made of anti-helium if BBN proceeded in a high $\bar{\eta}$ medium. Matter falling at the surface would annihilate and generate energy. An Earth size body would release 10^{49} ergs and could expel a shell of 0.01 $M_\odot$ in outer space at 10^4 km/s. Acceleration could take place in the resulting shock wave.

- Matching the $\overline{\mathrm{He}}$ flux, i.e. $\Phi_{\overline{\mathrm{He}}}/\Phi_{\mathrm{He}} \sim 10^{-8}$.

$$\Phi_{\overline{\mathrm{He}}} \simeq \frac{1}{4\pi}\frac{c}{V_{\mathrm{gal}}}\frac{f_{\overline{\mathrm{He}}} M_{\bar{*}}}{m_{\overline{\mathrm{He}}}} f_{\mathrm{acc}}$$

$$\Downarrow$$

$$\Phi_{\overline{\mathrm{He}}} \simeq 2\times 10^{-9}\,\mathrm{cm}^{-2}\,\mathrm{s}^{-1} \times \frac{M_{\bar{*}}}{\mathrm{M}_\odot} \times \frac{f_{\mathrm{acc}}}{10^{-6}}$$

- Once accelerated, CR $^4\overline{\mathrm{He}}$ need to cross over $20\,\mathrm{g\,cm}^{-2}$ of matter for being converted into $^3\overline{\mathrm{He}}$ in order to achieve the isotopic ratio $^4\overline{\mathrm{He}} : {}^3\overline{\mathrm{He}} = 1:3$

Table 2
Total reaction cross section, cross section for reactions with different number of charged prongs and for ^{3}He production. All quantities are in mb. $\langle n_c \rangle$ is the mean number of charged prongs per event.

Number of charged prongs	σ			N_{π^-}
	19.6 MeV	48.7 MeV	179.6 MeV	
^{3}He production	93.2 ± 7.9	58.6 ± 4.1	35.7 ± 2.8	

LEAR collaboration at CERN

Constraints on the antistar fraction in the Solar system neighborhood from the 10-years *Fermi* Large Area Telescope gamma-ray source catalog

S. Dupourqué, L. Tibaldo and P. von Ballmoos, Phys.Rev. **D103** (2021) 083016

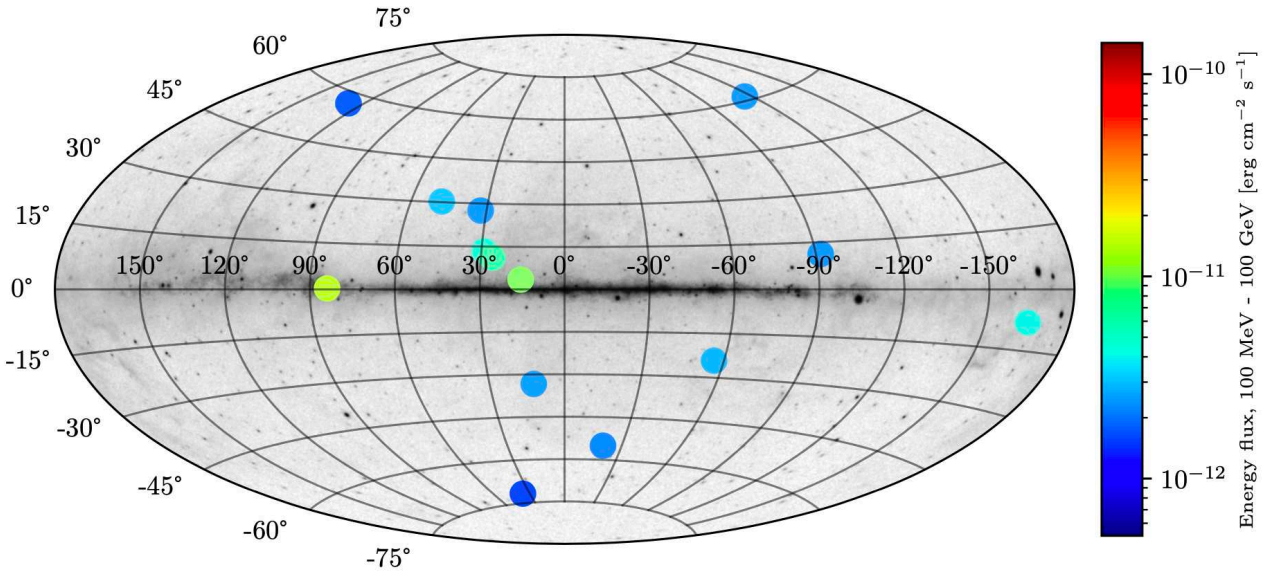

FIG. 1. Positions and energy flux in the 100 MeV - 100 GeV range of antistar candidates selected in 4FGL-DR2. Galactic coordinates. The background image shows the Fermi 5-year all-sky photon counts above 1 GeV (Image credit: NASA/DOE/Fermi LAT Collaboration)

$$f_{\bar{*}} \leq 2.68 \times 10^3 \left(\frac{\Phi_{\rm max}}{\rm cm^{-2}\ s^{-1}} \right)^{3/2} \left(\frac{\rho}{\rm m_p\ cm^{-3}} \right)^{-3/2} \left(\frac{M}{M_\odot} \right)^{-3} \left(\frac{\sqrt{v^2+c^2}}{10\ \rm km\ s^{-1}} \right)^{9/2}$$

Constraints on the antistar fraction in the Solar system neighborhood from the 10-years *Fermi* Large Area Telescope gamma-ray source catalog

S. Dupourqué, L. Tibaldo and P. von Ballmoos, Phys.Rev. **D103** (2021) 083016

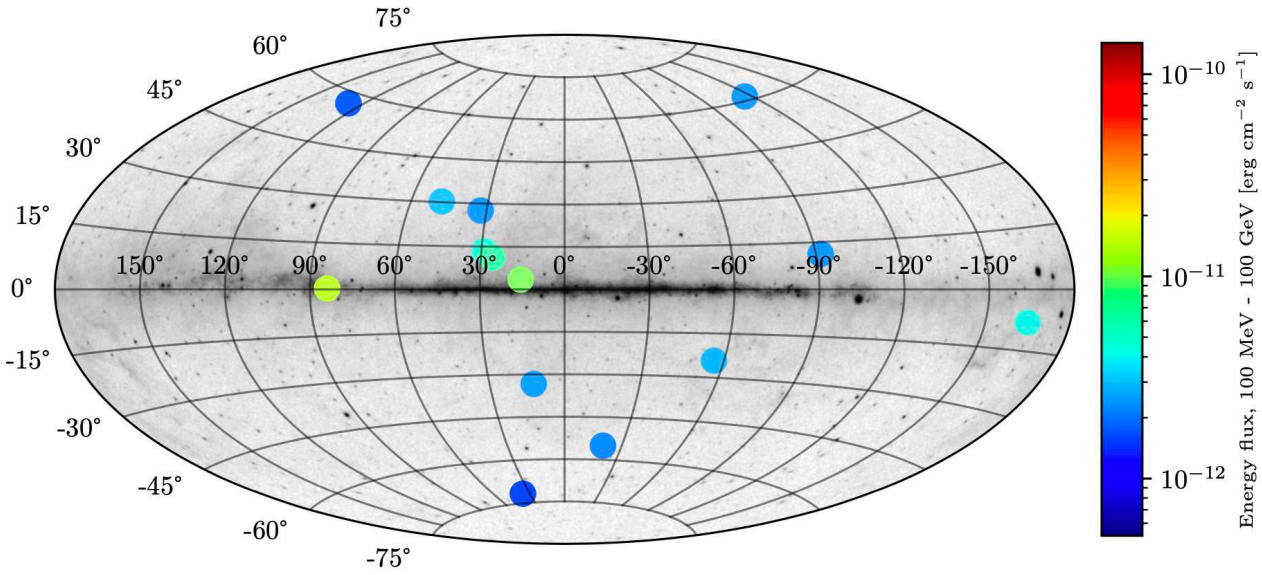

FIG. 1. Positions and energy flux in the 100 MeV - 100 GeV range of antistar candidates selected in 4FGL-DR2. Galactic coordinates. The background image shows the Fermi 5-year all-sky photon counts above 1 GeV (Image credit: NASA/DOE/Fermi LAT Collaboration)

$$f_{\bar{*}} \leq \boxed{10^{-8}} \left(\frac{\rho}{\mathrm{m}_p\ \mathrm{cm}^{-3}}\right)^{-3/2} \left(\frac{M}{M_\odot}\right)^{-3} \left(\frac{\sqrt{v^2+c^2}}{10\ \mathrm{km\ s}^{-1}}\right)^{9/2}$$

Anti-star velocities v may vary between 10 (disk–young) and 500 (halo–old) km/s

Anti-star genesis I – The Affleck-Dine mechanism

A new mechanism for baryogenesis

I. Affleck and M. Dine, Nucl. Phys. **B249** (1985) 361

In supersymmetric GUTs, supersymmetry is unbroken at high energies M of order M_G or M_P. The potential has flat directions along which scalar fields χ, possibly carrying baryon number B, can get large expectation values.

• SUSY is broken at a scale $\mu \sim \sqrt{m\,M}$, where $m \sim m_W$, by the potential

$$V(\chi) = m^2\,|\chi|^2 + V_{\not B}(\chi) \text{ where } V_{\not B}(\chi) = \lambda\left\{\chi^4 + \chi^{*4} + 2|\chi|^4\right\}$$

• For small values of $|\chi|$, the potential is approximately $U_B(1)$ symmetric and conserves the baryon number. The baryon density measures the orbital momentum of χ in its internal space

$$n_B(\chi) = iB\left\{\chi^*\partial_t\chi - \partial_t\chi^*\chi\right\} = -2B\dot{\theta}|\chi|^2 \text{ where } \chi = |\chi|e^{i\theta}$$

• At $T \sim \mu$, the expansion rate H becomes less than m and $\theta \sim mt \sim m/H$ starts to roll down the potential well. Depending on its initial position, χ may rotate, generating a non-vanishing baryon density. If $|\chi_0| \sim M$, we could get

$$n_B \sim B\,m M^2 \sim B\,n_\chi \text{ while } n_\gamma \sim \mu^3 \text{ and } n_B/n_\gamma \sim B\sqrt{M/m} \gg 1$$

• In AD original article, the coupling $\lambda \sim m^2/M^2$ and the baryon density and baryon-to-photon ratio are given by

$$n_B \sim \theta\,m|A(t)|^2\left\{\frac{|\chi_0|}{M}\right\}^2,\ n_\chi \sim m|A(t)|^2 \text{ and } n_B/n_\gamma \sim 10^2\,\theta\left\{\frac{|\chi_0|}{M}\right\}^2$$

Anti-star genesis I – The Affleck-Dine mechanism

A new mechanism for baryogenesis

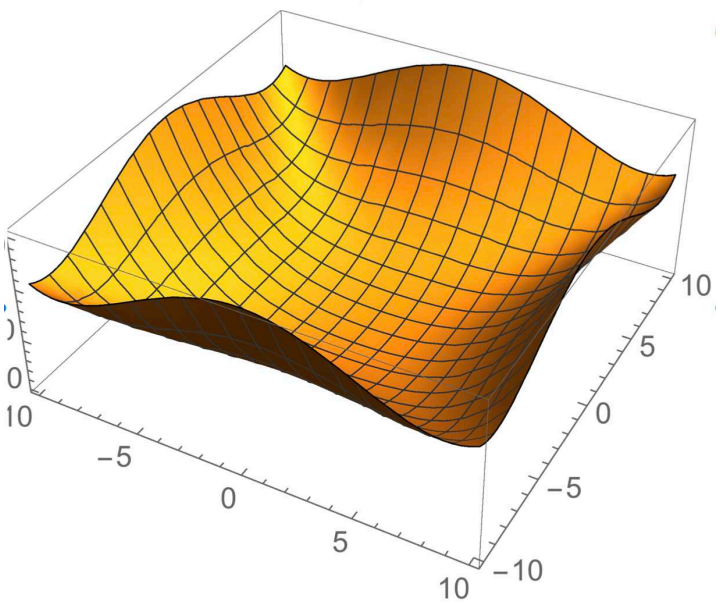

M. Drewes, in Light Anti-Nuclei as a Probe for New Physics, Leiden, 18/10/2019

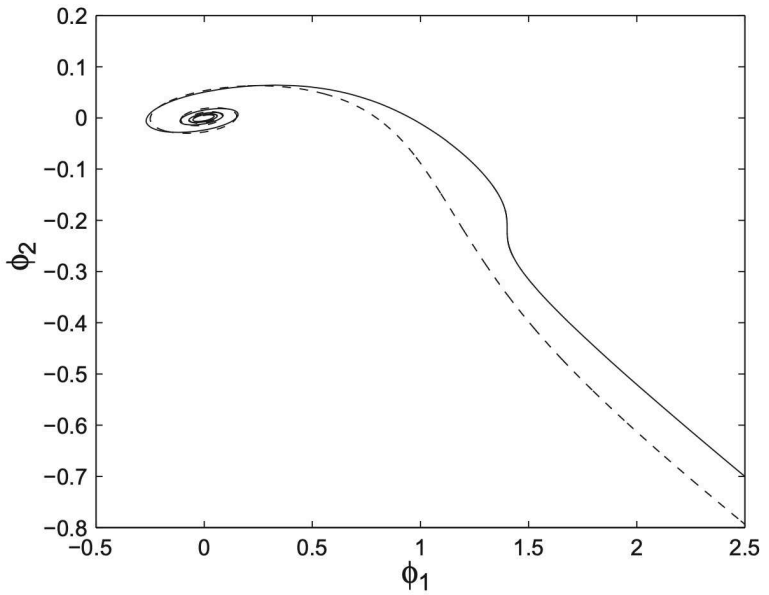

R. Allahverdi and A.Mazumdar, New Journal of Physics **14** (2012) 125013

• At $T\sim\mu$, the expansion rate H becomes less than m and $\theta\sim mt\sim m/H$ starts to roll down the potential well. Depending on its initial position, χ may rotate, generating a non-vanishing baryon density. If $|\chi_0|\sim M$, we could get

$$n_B\sim B\,m M^2\sim B\,n_\chi \text{ while } n_\gamma\sim\mu^3 \text{ and } n_B/n_\gamma\sim B\sqrt{M/m}\gg 1$$

• In AD original article, the coupling $\lambda\sim m^2/M^2$ and the baryon density and baryon-to-photon ratio are given by

$$n_B\sim\theta\,m|A(t)|^2\left\{\frac{|\chi_0|}{M}\right\}^2,\ n_\chi\sim m|A(t)|^2 \text{ and } n_B/n_\gamma\sim 10^2\,\theta\left\{\frac{|\chi_0|}{M}\right\}^2$$

Anti-star genesis II – The Dolgov-Silk scenario

Baryon isocurvature fluctuations at small scales and baryonic dark matter

A. Dolgov and J. Silk, Phys. Rev. **D47** (1993) 4244

In AD scenario, there is no control on the initial value χ_0 of the scalar field χ. Regions where n_B/n_γ is large should also have an astronomical size and feature a large variety in mass. That is why the AD baryogenesis takes place at the end of inflation.

• The scalar potential is chosen to contain a quartic term triggering a v.e.v. of $\mathcal{O}(\sigma)$

$$V(\chi) = m_{\rm eff}^2|\chi|^2 + \lambda|\chi|^4 \ln\frac{|\chi|^2}{\sigma^2} + V_{\not B}(\chi)$$

• The effective mass couples to the curvature R and to the inflaton field Φ. Temperature corrections come into play during reheating.

$$m_{\rm eff}^2 = m_0^2 + \xi R + \beta T^2 + \lambda_1(\Phi - \Phi_1)^2$$

• Towards the end of inflation, $\Phi = \Phi_1$ and a gate opens up for χ to transition from 0 to σ. A first order phase transition starts. Bubbles appear inside which $|\chi| \sim \sigma$. Very rapidly, the gate closes and χ relaxes to 0. Depending on the position of χ in the complex plane, these bubbles can contain a large baryonic charge.

• This scenario leads to the formation of macroscopic regions containing large amounts of baryons or anti-baryons. At the QCD transition, numerous heavy baryons form inside these regions which become matter or antimatter objects such as gas clouds, dense stars and even black holes depending on their mass M and their baryon asymmetry.

$$\frac{dn}{dM} \propto \exp\left\{-\gamma \ln^2(M/M_0)\right\}$$

Anti-star genesis II – The Dolgov-Silk scenario

Baryon isocurvature fluctuations at small scales and baryonic dark matter

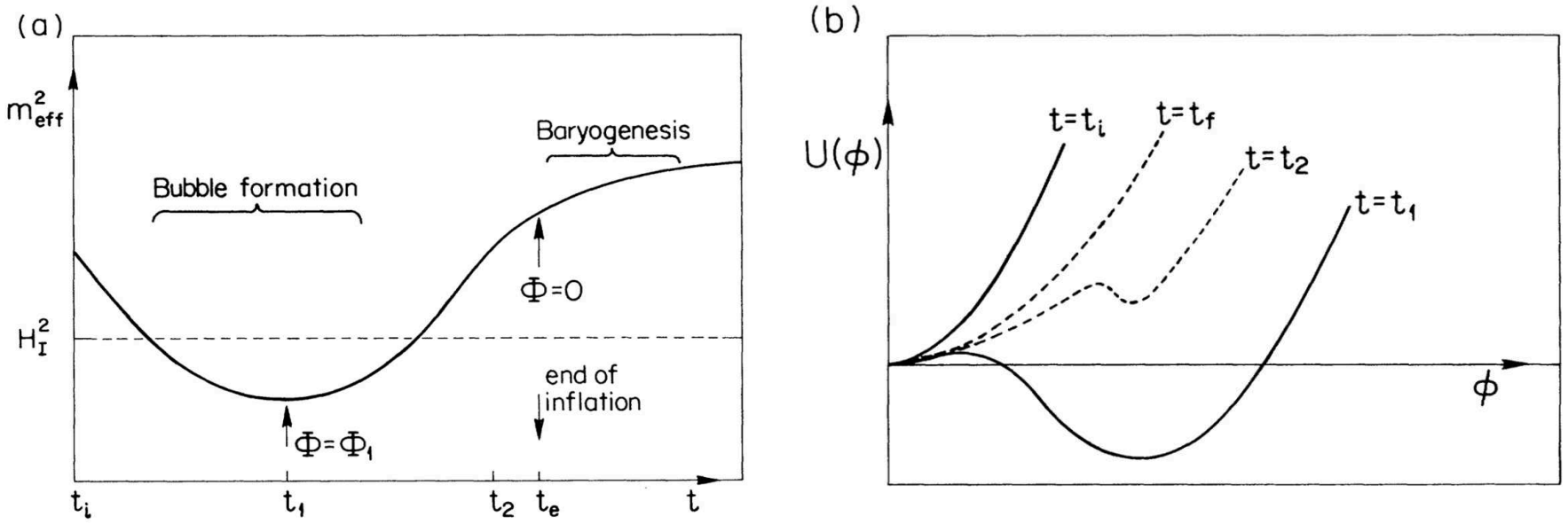

• Towards the end of inflation, $\Phi = \Phi_1$ and a gate opens up for χ to transition from 0 to σ. A first order phase transition starts. Bubbles appear inside which $|\chi| \sim \sigma$. Very rapidly, the gate closes and χ relaxes to 0. Depending on the position of χ in the complex plane, these bubbles can contain a large baryonic charge.

• This scenario leads to the formation of macroscopic regions containing large amounts of baryons or anti-baryons. At the QCD transition, numerous heavy baryons form inside these regions which become matter or antimatter objects such as gas clouds, dense stars and even black holes depending on their mass M and their baryon asymmetry.

$$\frac{dn}{dM} \propto \exp\left\{-\gamma \ln^2(M/M_0)\right\}$$

Takeaway

- Anti-helium-3 and anti-helium-4 candidates may have been identified by AMS-02.
  Massive background simulations are carried out to evaluate significance.
  No $\overline{\text{He}}$ found but MC simulations are difficult to validate.

- $^3\overline{\text{He}}$ events
  Unless CR propagation and coalescence are very different from expected,
  AMS-02 should **not** see secondary CR $^3\overline{\text{He}}$.
  Interesting possibility from DM annihilating into $\bar{\Lambda}_b$ mesons – Linden & Winkler.

- $^4\overline{\text{He}}$ events
  There is no hope to detect a single event from CR spallation or DM.
  If confirmed, a single $^4\overline{\text{He}}$ would be a major discovery.

- Observation of $^3\overline{\text{He}}$ and $^4\overline{\text{He}}$ events would imply a drastic revision of cosmology and would request a more fundamental theory than the standard model of particle physics. A few routes have already been explored.

Thanks for your attention

Constraints on the antistar fraction in the Solar system neighborhood from the 10-years *Fermi* Large Area Telescope gamma-ray source catalog

S. Dupourqué, L. Tibaldo and P. von Ballmoos, Phys.Rev. **D103** (2021) 083016

- extended sources are excluded since the angular size of a star is several orders of magnitude smaller than the LAT resolution at low energy, thus antistars are expected to be point-like sources;

- sources associated with objects known from other wavelengths that belong to established gamma-ray source classes (e.g., pulsars, active galactic nuclei) are excluded;

- sources with total TS summed for energy bands above 1 GeV larger than 9 (that is, emission detected at $> 3\sigma$ above 1 GeV) are excluded since the emission spectrum from proton-antiproton annihilation is null above 938 MeV (mass of the proton); the high-energy cutoff makes it possible to differentiate the matter-antimatter annihilation signal from the well-known pion-bump signal produced by interactions of cosmic rays with an approximate power-law spectrum onto the ISM and seen in the Galactic interstellar emission and a few supernova remnants [23, 24]; to our knowledge this is the first time that spectral criteria are used to select candidate antistars in gamma-ray catalogs;

- sources flagged in the catalog as potential spurious detections related to uncertainties in the background models or nearby bright sources (flags 1 to 6) are excluded.

6) Anti-clouds – a (crazy) step further

Taken at face value, the isotopic ratio of $\overline{\text{He}}$ nuclei could be explained by anisotropic BBN taking place in regions where $\bar{\eta} \sim (1.3 - 6) \times 10^{-13}$.

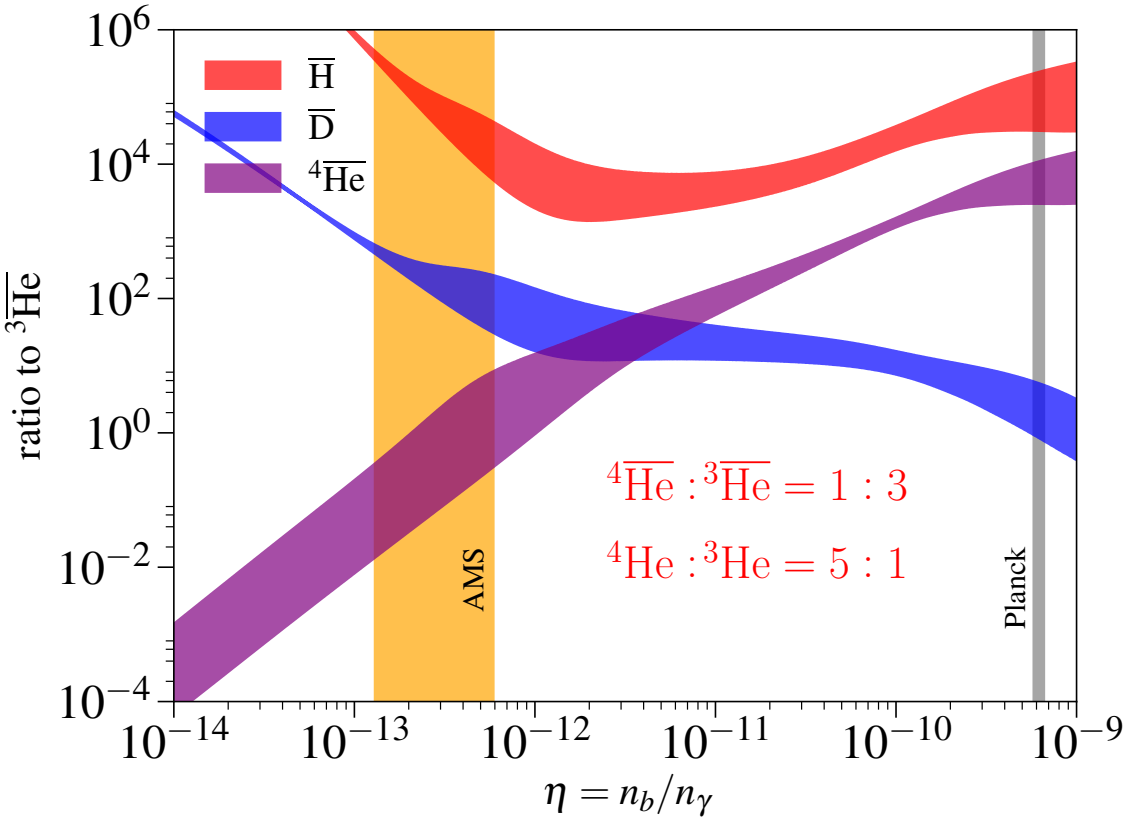

$$10^{-8} \simeq \frac{\Phi_{\overline{\text{He}}}}{\Phi_{\text{He}}} \simeq \frac{N_{\overline{\text{He}}}}{N_{\text{He}}} = \frac{V_{\bar{\text{M}}}}{V_{\text{M}}} \frac{n_{\overline{\text{He}}}}{n_{\text{He}}} = \frac{V_{\bar{\text{M}}}}{V_{\text{M}}} \frac{n_{\bar{b}}}{n_b} \frac{n_{\overline{\text{He}}}}{n_{\overline{\text{H}}}} \frac{n_{\text{H}}}{n_{\text{He}}} \quad \text{in ISM}$$

$$\Downarrow$$

$$\left.\frac{V_{\bar{\text{M}}}}{V_{\text{M}}} \frac{n_{\bar{b}}}{n_b}\right|_{\text{ISM}} \simeq 10^{-8} \times 10^{-1} \times \left(10^4 - 10^{5.5}\right) \simeq \left(10^{-5} - 10^{-3.5}\right)$$

γ-ray line constraint at 933 MeV on $n_p^{\rm local}$

Annihilations inside anti-matter domains yield γ-ray lines. We are interested here in $p\,\bar{p} \to \pi^0\,\gamma$ at 933 MeV whose integrated flux over the MW is constrained by Fermi-LAT observations.

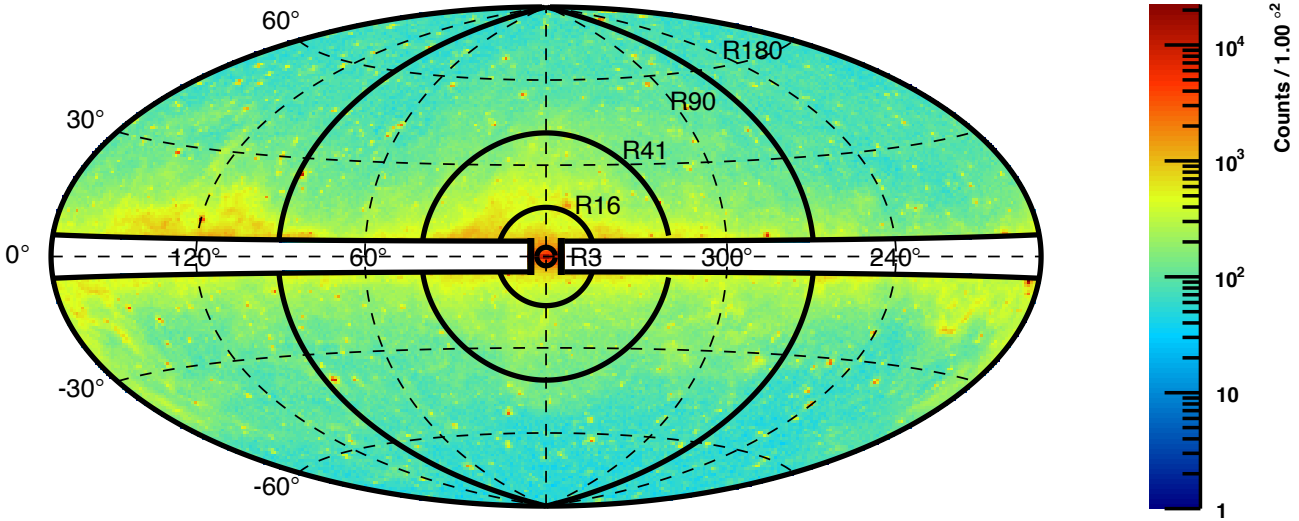

M. Ackermann et al. (Fermi-LAT), Phys. Rev. **D91** (2015) 122002

$$\left.\frac{{\rm d}^2 N_\gamma}{{\rm d}V\,{\rm d}t}\right|_{\pi^0\gamma} = \rho^{\rm ISM}_{\pi^0\gamma} = \mathcal{B}_{\pi^0\gamma} \left\{\frac{V_{\overline{\rm M}}}{V_{\rm M}}\right\} n_{\bar{p}}\, n_p^{\rm local}\, \langle\sigma_{p\bar{p}} v\rangle$$

$$\Phi_\gamma = \tfrac{1}{4\pi}\int^{R180} {\rm d}\ell\, d\Omega\, \rho^{\rm ISM}_{\pi^0\gamma} \;\leq\; 6.87\times10^{-7}\,{\rm cm}^{-2}\,{\rm s}^{-1}\ \text{(Fermi-LAT)}$$

$$\Downarrow$$

$$n_p^{\rm local} \lesssim \left(10^{-10} - 3\times10^{-9}\right)\ {\rm cm}^{-3}$$

This is O(10) times better than the lifetime limit

γ-rays from cosmic-ray annihilations in close-by anti-clouds

Nothing prevents cosmic-ray protons to penetrate inside anti-clouds where they annihilate.This should yield a strong annihilation signal appearing as **(i)** a continuous emission and also as **(ii)** a point source in the sky if anti-matter domains are well localized in space.

We start from $N_{\bar{c}}\, M_{\bar{c}} = M_{\overline{\rm M}} = m_{\bar{b}}\, n_{\bar{b}}\, V_{\overline{\rm M}}$

and assume that $N_{\bar{c}} \times 2h\, D_{\bar{c}}^2 = V_{\rm M} \equiv V_{\rm disk}$ (homogeneous over MW)

$$\Downarrow$$

$$2h\, D_{\bar{c}}^2 = \frac{V_{\rm M}}{N_{\bar{c}}} = \frac{V_{\rm M}\, n_b}{V_{\overline{\rm M}}\, n_{\bar{b}}} \times \frac{M_{\bar{c}}}{n_b\, m_{\bar{b}}}$$

$$\Downarrow$$

$$D_{\bar{c}} \simeq (1 \text{ to } 5.5) \times 860\,{\rm pc} \times \left\{ \frac{M_{\bar{c}}}{10^3\,{\rm M}_\odot} \right\}^{1/2}$$

γ-rays from cosmic-ray annihilations in close-by anti-clouds

Nothing prevents cosmic-ray protons to penetrate inside anti-clouds where they annihilate.This should yield a strong annihilation signal appearing as **(i)** a continuous emission and also as **(ii)** a point source in the sky if anti-matter domains are well localized in space.

The absolute luminosity of a cloud is its production rate of photons

$$L_\gamma = \int_{E_p^{\rm inf}}^{E_p^{\rm sup}} \langle \sigma_{p\bar{p}} v \rangle \, n_{\bar{p}} \, \frac{dn_p}{dE_p} \, dE_p \times \mathcal{B}_\gamma^{\rm eff} \times V_{\bar{c}} \propto M_{\bar{c}}$$

$$\Downarrow$$

$$\Phi_\gamma = \frac{L_\gamma}{4\pi D_{\bar{c}}^2} = \frac{\mathcal{B}_\gamma^{\rm eff}}{D_{\bar{c}}^2} \times \frac{M_{\bar{c}}}{m_{\bar{p}}} \times \int_{E_p^{\rm inf}}^{E_p^{\rm sup}} \sigma_{p\bar{p}} \, \Phi_p(E_p) \, dE_p$$

The flux does not depend on $M_{\bar{c}}$. Assuming $\mathcal{B}_\gamma^{\rm eff} = 4 \times 4\%$ and integrating E_p from 3 to 10 GeV for photons in the 1–3 GeV energy band, we get

$$\Phi_\gamma^{\rm cloud} \simeq (0.03 \text{ to } 1) \times 10^{-10} \, {\rm cm}^{-2} \, {\rm s}^{-1}$$

$$\text{to be compared to } \Phi_\gamma^{\rm Fermi} \geq 10^{-10} \, {\rm cm}^{-2} \, {\rm s}^{-1}$$

Clouds may be on the verge of detection

7) Matter-antimatter segregation is a problem

- The Quark/Hadron phase transition takes place between 100 and 200 MeV. Lattice QCD indicates that it might be 2nd order.

$$\mathrm{u, d, s, g} \Rightarrow \pi^0, \pi^{\pm} \text{ and traces of } p, n \;\&\; \bar{p}, \bar{n}$$

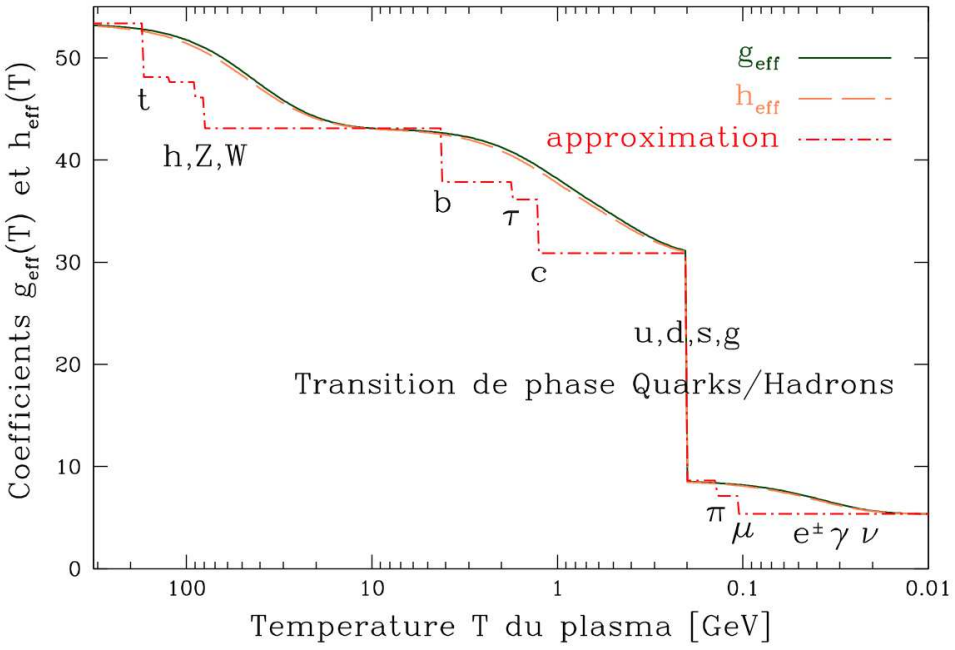

- As soon as they are formed, nucleons and antinucleons annihilate.

$$N + \bar{N} \rightleftharpoons \pi + \bar{\pi}$$

- Assuming **no asymmetry** between N & $\bar{N}$, their densities are equal. Codensities are defined as $\tilde{n}_N \equiv n_N/T^3$ and $\tilde{n}_{\bar{N}} \equiv n_{\bar{N}}/T^3$.

$$\frac{d\tilde{n}_N}{dt} + \{\langle\sigma_{\rm an}v\rangle n_N\}\,\tilde{n}_N = \langle\sigma_{\rm an}v\rangle T^3\,{\tilde{n}_N^{\rm e}}^2$$

$$\tau_{\rm rel}^{-1} \equiv \Gamma_{\rm rel} = \langle\sigma_{\rm an}v\rangle n_A \qquad\qquad \tau_{\rm eq}^{-1} \equiv \Gamma_{\rm eq} = -\frac{d\ln(\langle\sigma_{\rm an}v\rangle T^3\,{\tilde{n}_A^{\rm e}}^2)}{dt}$$

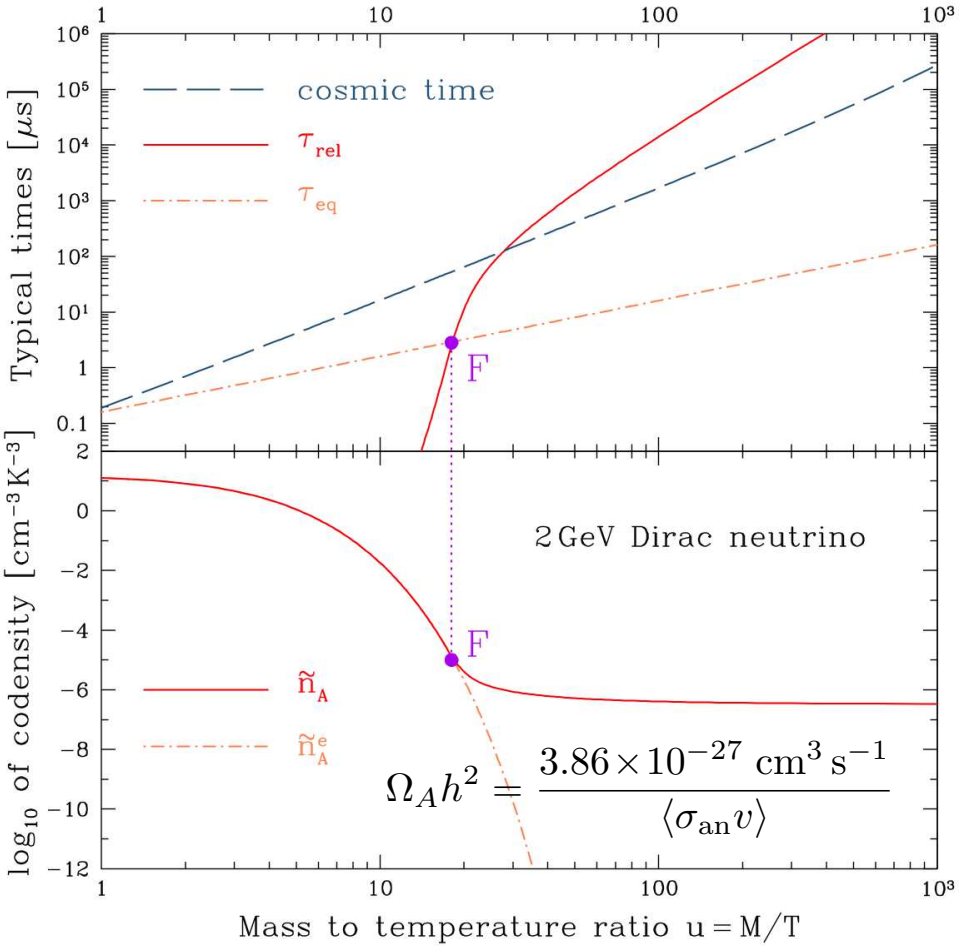

- Annihilation of N & $\bar{N}$ proceeds very strongly with freeze-out at $u_{\rm F} = 41.8$ and $T_{\rm F} \simeq 22$ MeV.
  Nucleons and antinucleons are completely depleted.

$$\frac{n_N^0}{n_\gamma} \equiv \frac{\tilde{n}_N^0}{\tilde{n}_\gamma} = \frac{2\pi^2}{\zeta(3)} \left\{ \frac{1}{1+2u_{\rm F}} \right\} \left\{ \frac{u_{\rm F}}{2\pi} \right\}^{3/2} e^{-u_{\rm F}} \simeq 2.34 \times 10^{-18}$$

$$\Uparrow$$

$$\langle \sigma_{\rm an} v \rangle \simeq \left\{ \sigma_{\rm an} = 10^{-25}\ {\rm cm}^2 \right\} \times \left\{ v_{\rm B} = c\sqrt{3/u} \right\}$$

- Annihilation of N & $\bar{N}$ proceeds very strongly with freeze-out at $u_{\rm F} = 41.8$ and $T_{\rm F} \simeq 22$ MeV.
  Nucleons and antinucleons are completely depleted.

$$\frac{n_N^0}{n_\gamma} \equiv \frac{\tilde{n}_N^0}{\tilde{n}_\gamma} = \frac{2\pi^2}{\zeta(3)} \left\{ \frac{1}{1+2u_{\rm F}} \right\} \left\{ \frac{u_{\rm F}}{2\pi} \right\}^{3/2} e^{-u_{\rm F}} \simeq 2.34 \times 10^{-18}$$

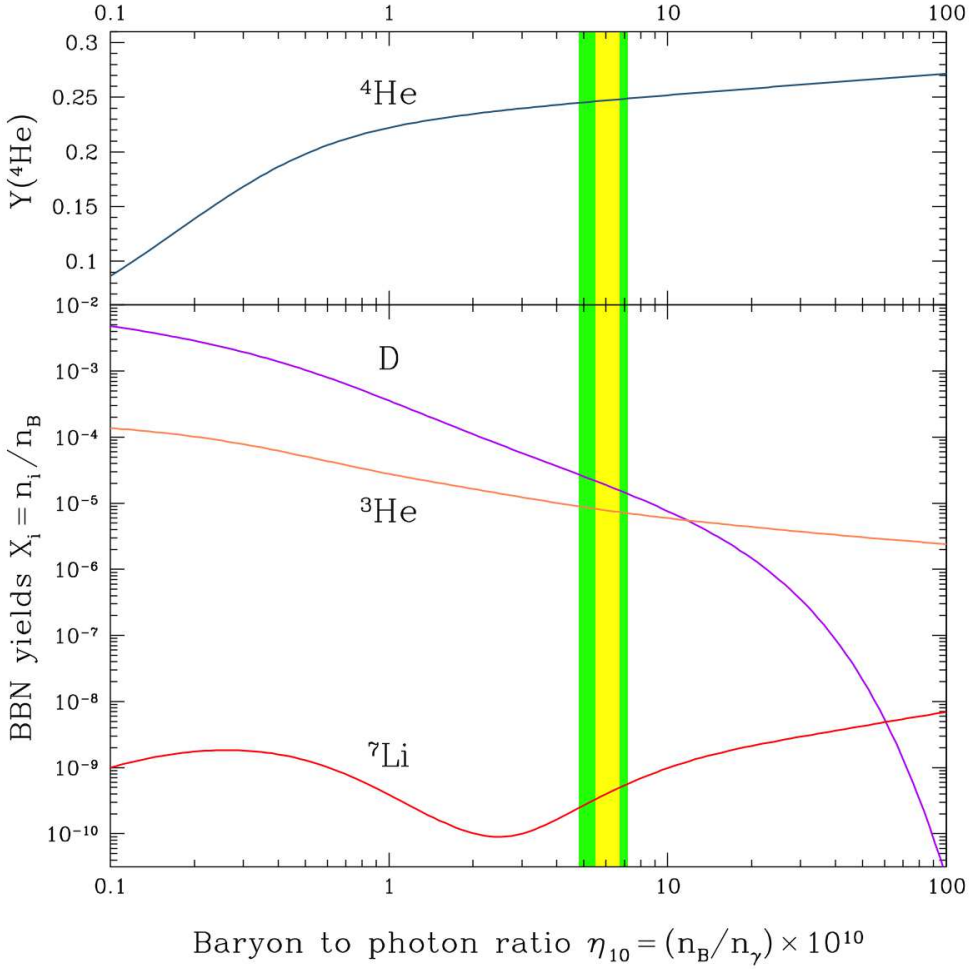

- Annihilation of N & $\bar{N}$ proceeds very strongly with freeze-out at $u_{\rm F} = 41.8$ and $T_{\rm F} \simeq 22$ MeV.
  Nucleons and antinucleons are completely depleted.

$$\frac{n_N^0}{n_\gamma} \equiv \frac{\tilde{n}_N^0}{\tilde{n}_\gamma} = \frac{2\pi^2}{\zeta(3)} \left\{ \frac{1}{1+2u_{\rm F}} \right\} \left\{ \frac{u_{\rm F}}{2\pi} \right\}^{3/2} e^{-u_{\rm F}} \simeq 2.34 \times 10^{-18}$$

$$\Uparrow$$

$$\langle \sigma_{\rm an} v \rangle \simeq \left\{ \sigma_{\rm an} = 10^{-25}\ {\rm cm}^2 \right\} \times \left\{ v_{\rm B} = c\sqrt{3/u} \right\}$$

- Segregation between N & $\bar{N}$ must take place **before** freeze-out at $u_{\rm S} = 25.1$, $T_{\rm S} \simeq 37.4$ MeV and cosmic time $t_{\rm S} \simeq 0.5$ ms.

$$\left. \frac{n_N^{\rm e}}{n_\gamma} \right|_{\rm S} \equiv \left. \frac{\tilde{n}_N^{\rm e}}{\tilde{n}_\gamma} \right|_{\rm S} = \frac{2\pi^2}{\zeta(3)} \left\{ \frac{u_{\rm S}}{2\pi} \right\}^{3/2} e^{-u_{\rm S}} \simeq 1.65 \times 10^{-9}$$

$$\Downarrow$$

$$\mathcal{M}_N = M_p\, n_N\, R_{\rm S}^3 \simeq 1.79 \times 10^{22}\ {\rm kg}$$

$$\Downarrow$$

Segregation active since then

We have no idea on how it proceeds

8) The standard lore or Sakharov's prescription

- In June 1933, Wolfgang Pauli sends a letter to Werner Heisenberg where he gives his opinion on Dirac's theory:

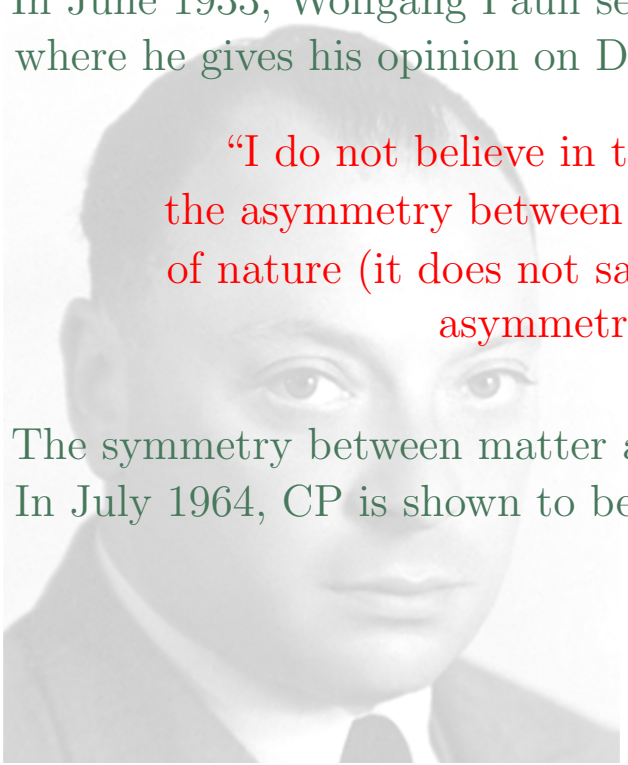

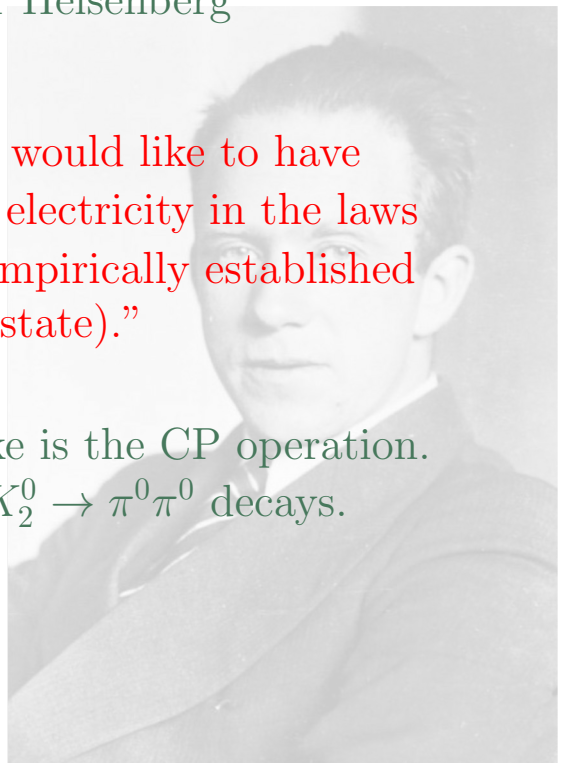

"I do not believe in the hole theory, since I would like to have the asymmetry between positive and negative electricity in the laws of nature (it does not satisfy me to shift the empirically established asymmetry to one of the initial state)."

- The symmetry between matter and antimatter at stake is the CP operation. In July 1964, CP is shown to be violated with a few $K_2^0 \to \pi^0\pi^0$ decays.

VOLUME 13, NUMBER 4 PHYSICAL REVIEW LETTERS 27 JULY 1964

EVIDENCE FOR THE 2π DECAY OF THE K_2^0 MESON*†

J. H. Christenson, J. W. Cronin,‡ V. L. Fitch,‡ and R. Turlay§
Princeton University, Princeton, New Jersey
(Received 10 July 1964)

8) The standard lore or Sakharov's prescription

- In June 1933, Wolfgang Pauli sends a letter to Werner Heisenberg where he gives his opinion on Dirac's theory:

"I do not believe in the hole theory, since I would like to have the asymmetry between positive and negative electricity in the laws of nature (it does not satisfy me to shift the empirically established asymmetry to one of the initial state)."

- The symmetry between matter and antimatter at stake is the CP operation. In July 1964, CP is shown to be violated with a few $K_2^0 \to \pi^0\pi^0$ decays.

Remarque !

$$\text{sous } CP : \mathrm{u_L} \Leftrightarrow \bar{\mathrm{u}}_\mathrm{R} \text{ et } \mathrm{d_L} \Leftrightarrow \bar{\mathrm{d}}_\mathrm{R}$$

$$(1+i\varepsilon)\,\bar{\mathrm{u}}_\mathrm{R}\gamma_\mu \mathrm{d_L}\, W^\mu \xrightarrow{CP} (1+i\varepsilon)\,\bar{\mathrm{d}}_\mathrm{R}\gamma_\mu \mathrm{u_L}\, W^\mu$$

$$(1+i\varepsilon)\,\bar{\mathrm{u}}_\mathrm{R}\gamma_\mu \mathrm{d_L}\, W^\mu \xrightarrow{h.c.} (1-i\varepsilon)\,\bar{\mathrm{d}}_\mathrm{R}\gamma_\mu \mathrm{u_L}\, W^\mu$$

Si $\varepsilon \neq 0 \Rightarrow$, violation de CP !

We would conclude therefore that K_2^0 decays to two pions with a branching ratio $R = (K_2 \to \pi^+ + \pi^-)/(K_2^0 \to \text{all charged modes}) = (2.0 \pm 0.4) \times 10^{-3}$ where the error is the standard deviation. As emphasized above, any alternate explanation of the effect requires highly nonphysical behavior of the three-body decays of the K_2^0. The presence of a two-pion decay mode implies that the K_2^0 meson is not a pure eigenstate of CP. Expressed as $K_2^0 = 2^{-1/2}[(K_0 - \bar{K}_0) + \epsilon(K_0 + \bar{K}_0)]$ then $|\epsilon|^2 \cong R_T \tau_1 \tau_2$ where τ_1 and τ_2 are the K_1^0 and K_2^0 mean lives and R_T is the branching ratio including decay to two π^0. Using $R_T = \frac{3}{2}R$ and the branching ratio quoted above, $|\epsilon| \cong 2.3 \times 10^{-3}$.

Baryogenesis and Sakharov's prescription

- Interactions violate the baryon number B.
- Interactions violate CP symmetry.
- Baryogenesis acts out of thermal equilibrium.

Baryogenesis and Sakharov's prescription

- Interactions violate the baryon number B.
- Interactions violate CP symmetry.
- Baryogenesis acts out of thermal equilibrium.

$$\mathcal{M}(i \to j) = \mathcal{M}(\bar{j} \to \bar{i}), \qquad (CPT \text{ invariance})$$

$$\sum_j |\mathcal{M}(i \to j)|^2 = \sum_j |\mathcal{M}(j \to i)|^2 , \qquad (\text{unitarity})$$

$$\sum_j |\mathcal{M}(i \to j)|^2 = \sum_j |\mathcal{M}(j \to \bar{i})|^2 = \sum_j |\mathcal{M}(j \to i)|^2 , \qquad (CPT + \text{unitarity})$$

$$\mathcal{M}(i \to j) = \mathcal{M}(\bar{i} \to \bar{j}) = \mathcal{M}(j \to i), \qquad (CP \text{ invariance})$$

A simplistic model

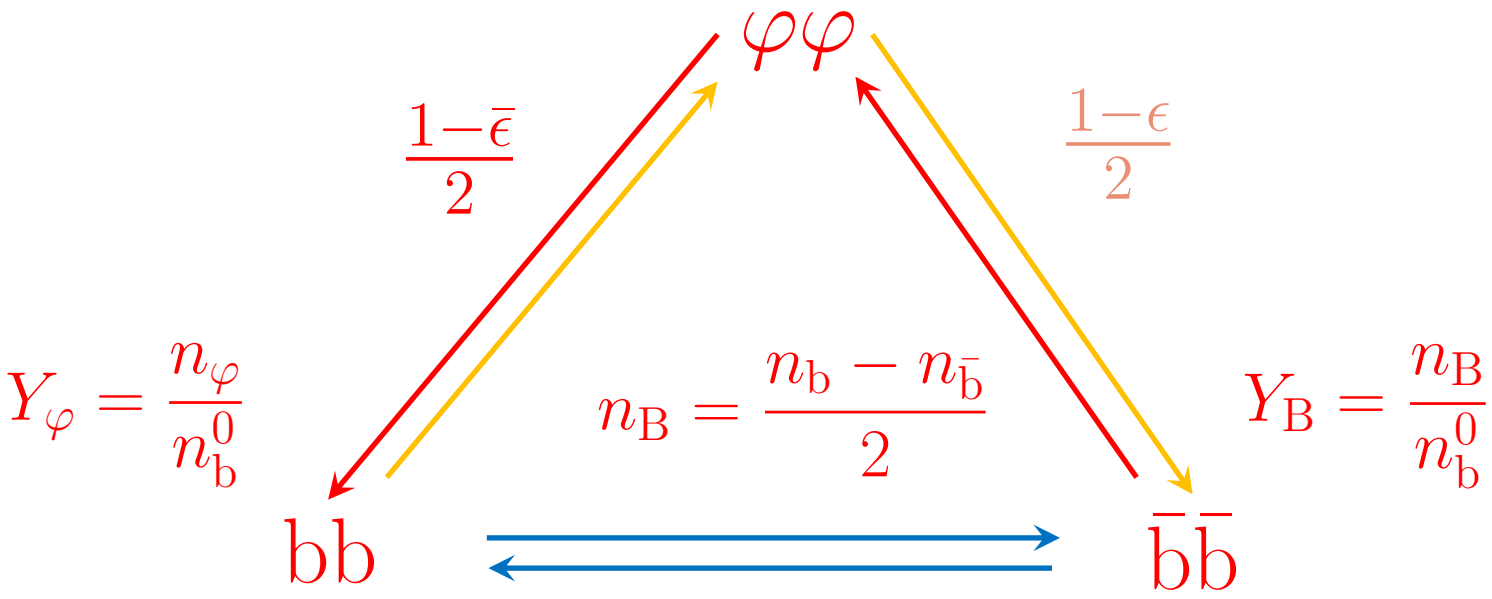

$$\left|\mathcal{M}(\varphi\varphi \to {\rm bb}\right|^2 = \left|\mathcal{M}(\bar{\rm b}\bar{\rm b} \to \varphi\varphi\right|^2 = \left[\mathcal{M}_0\right|^2 \left(\tfrac{1-\bar{\epsilon}}{2}\right)$$

$$\left|\mathcal{M}(\varphi\varphi \to \bar{\rm b}\bar{\rm b}\right|^2 = \left|\mathcal{M}({\rm bb} \to \varphi\varphi\right|^2 = \left[\mathcal{M}_0\right|^2 \left(\tfrac{1-\epsilon}{2}\right)$$

$$k_{\bar{\rm b}} \left|\mathcal{M}({\rm bb} \to \bar{\rm b}\bar{\rm b})\right|^2 + k_\varphi \left|\mathcal{M}({\rm bb} \to \varphi\varphi)\right|^2 \equiv k_{\rm b} \left|\mathcal{M}(\bar{\rm b}\bar{\rm b} \to {\rm bb})\right|^2 + k_\varphi \left|\mathcal{M}(\bar{\rm b}\bar{\rm b} \to \varphi\varphi)\right|^2$$

$$\frac{dY_\varphi}{dt} = -\langle\sigma_0 v\rangle n_{\rm b}^0 \left\{1 - \left(\tfrac{\epsilon+\bar{\epsilon}}{2}\right)\right\} \left\{Y_\varphi^2 - \left(Y_\varphi^{\rm e}\right)^2\right\} + \langle\sigma_0 v\rangle n_{\rm b}^0 \left(\bar{\epsilon} - \epsilon\right) \left(Y_\varphi^{\rm e}\right)^2 Y_{\rm B}$$

$$\frac{dY_{\rm B}}{dt} = \langle\sigma_0 v\rangle n_{\rm b}^0 \left(\tfrac{\epsilon-\bar{\epsilon}}{4}\right) \left\{Y_\varphi^2 - \left(Y_\varphi^{\rm e}\right)^2\right\} - \langle\sigma_0 v\rangle n_{\rm b}^0 \left\{1 - \left(\tfrac{\epsilon+\bar{\epsilon}}{2}\right)\right\} \left(Y_\varphi^{\rm e}\right)^2 Y_{\rm B} - 2\langle\sigma_0 v\rangle n_{\rm b}^0 Y_{\rm B}$$